

T-2168

A MAGNETIC INVESTIGATION OF
MOUNT HOOD, OREGON

by
Guy Flanagan

ProQuest Number: 11016548

All rights reserved

INFORMATION TO ALL USERS

The quality of this reproduction is dependent upon the quality of the copy submitted.

In the unlikely event that the author did not send a complete manuscript and there are missing pages, these will be noted. Also, if material had to be removed, a note will indicate the deletion.



ProQuest 11016548

Published by ProQuest LLC (2019). Copyright of the Dissertation is held by the Author.

All rights reserved.

This work is protected against unauthorized copying under Title 17, United States Code
Microform Edition © ProQuest LLC.

ProQuest LLC.
789 East Eisenhower Parkway
P.O. Box 1346
Ann Arbor, MI 48106 – 1346

A thesis submitted to the Faculty and the Board of Trustees of the Colorado School of Mines in partial fulfillment of the requirements for the degree of Master of Science, Geophysics.

Golden, Colorado

Date April 2, 1979

Signed: Guy Flanagan
Guy Flanagan

Approved: David Butler

Thesis Advisor

Dr. D.L. Butler

Golden, Colorado

Date April 2, 1979

George V. Keller

Head of Department

Dr. G.V. Keller

ABSTRACT

A qualitative assessment of an aeromagnetic survey flown in May, 1977 over the Mount Hood area of Oregon indicates that the aeromagnetic anomaly pattern is controlled to a large extent by the topographic expression of the area's highly magnetized Cenozoic volcanics.

Three-dimensional magnetic modeling of the Mount Hood volcanic cone indicates that the main bulk of the cone, above approximately 1650 meters elevation, is composed of magnetically similar andesites. These andesites are magnetized in a direction ($I=80.0^\circ$, $D=28.3^\circ$) close to that of the present earth's field ($I=68.5^\circ$, $D=20.3^\circ$), and with a magnetization of 2.9 A/m. The chief exception to this is the remains of the Sandy Glacier Volcano which outcrops on the northwest slope of the Mount Hood cone. Calculations show that this old basaltic cone is magnetized with a direction approximately opposite to the present Earth's field and with a magnitude of magnetization of 3.9 A/m.

The Sandy Glacier Volcano comprises approximately one-tenth of the total volume of the Mount Hood volcanic cone above 1650 meters elevation. This result indicates that the Sandy Glacier Volcano is probably much younger than the 3.2 million years previously supposed.

TABLE OF CONTENTS

Introduction	1
Geology	5
Late Miocene Deposits	5
Yakima Basalt	5
Rhododendron Formation	6
Dalles Formation	7
Pliocene Deposits	8
Quaternary Deposits	12
Outlying Deposits	12
Mount Hood Volcano	13
The Aeromagnetic Data	16
Data Processing	16
Transformations of the Aeromagnetic Data ...	19
Upward Continuation	20
Integration	22
Reduction-to-the-Pole	24
Laboratory and Field Work	28
Measurement of Remnant Magnetization and	
Susceptibility	28
Analysis of Results	29
Qualitative Analysis	37

Modeling	42
Initial Least-Squares Modeling	43
Modeling Program Input	44
Initial Modeling Results	47
The Refined Model	51
Conclusions	61
Bibliography	63

LIST OF FIGURES

Figure 1	Index map of the Cascade andesitic stratocone volcanos.	2
Figure 2	The low-level aeromagnetic survey of the flanks of Mount Hood and the surrounding area.	17
Figure 3	The high-level aeromagnetic survey of the Mount Hood volcanic cone.	18
Figure 4	The upward continued version of the low-level aeromagnetic survey.	21
Figure 5	The integrated version of the Mount Hood aeromagnetics.	23
Figure 6	The reduced-to-the-pole version of the low-level aeromagnetic survey.	25
Figure 7	The reduced-to-the-pole version of the integrated Mount Hood aeromagnetics.	26
Figure 8	Topographic model of the Mount Hood cone.	46
Figure 9	Residual from the 16 layer least-squares best-fit model of the entire Mount Hood cone anomaly ($I=70.9^\circ$, $D=-0.6^\circ$).	50
Figure 10	Projection of the Sandy Glacier Volcano model onto the topography of the Mount Hood cone.	53
Figure 11	Residual from the refined modeling of the Sandy Glacier Volcano ($I=-63.9^\circ$, $D=180.0^\circ$, and $J=6.5$ A/m) and Mount Hood cone ($I=80.0^\circ$, $D=28.3^\circ$, and $J=2.9$ A/m).	55
Figure 12	Residual from the refined modeling of the Sandy Glacier Volcano ($I=-55.0^\circ$, $D=190.0^\circ$, and $J=6.9$ A/m) and Mount Hood cone ($I=76.4^\circ$, $D=27.6^\circ$, and $J=2.9$ A/m).	58

LIST OF PLATES

- Plate 1 Geology of the Mount Hood area, Oregon.
- Plate 1a Mount Hood Oregon: Topography
- Plate 2 Mount Hood Oregon: Low-level aeromagnetics.
- Plate 3 Mount Hood Oregon: High-level aeromagnetics.
- Plate 4 Mount Hood Oregon: Low-level aeromagnetics upward continued.
- Plate 5 Mount Hood Oregon: Integrated aeromagnetics.
- Plate 6 Mount Hood Oregon: Low-level aeromagnetics reduced-to-the-pole.
- Plate 7 Mount Hood Oregon: Integrated aeromagnetics reduced-to-the-pole.

LIST OF TABLES

- | | | |
|---------|---|----|
| Table 1 | Laboratory results on Mount Hood andesites. | 31 |
| Table 2 | Laboratory results on crater area rocks. | 32 |
| Table 3 | Laboratory results on the Sandy Glacier Volcano. | 33 |
| Table 4 | Laboratory results on basalts from Dog River Springs. | 34 |
| Table 5 | Laboratory results on rock samples. | 35 |
| Table 6 | Least-squares best-fit magnetization inversions. | 48 |

ACKNOWLEDGEMENTS

I would like to thank the members of my thesis committee; Dr. George V. Keller, Dr. Catherine K. Skokan and especially my thesis advisor Dr. David L. Butler for their assistance in this work. Special thanks go to the fourth member of my committee, Dr. David L. Williams of the United States Geological Survey's Regional Geophysics Branch. His assistance and cooperation in allowing me to use the Mount Hood aeromagnetics as a basis for my thesis is deeply appreciated.

I would also like to acknowledge the assistance of Craig White of the University of Oregon for his help in collecting and identifying rock samples, and Mike Webring of the United States Geological Survey's Regional Geophysics Branch for his patience in answering my many questions regarding the use of the Geological Survey's computer system.

I wish to also acknowledge that this work was supported by the United States Geological Survey's project no. 9730-01721.

INTRODUCTION

Mount Hood, located in north-central, Oregon (Fig. 1), is a Late Pleistocene to Recent volcanic cone rising 2400 meters above the surrounding terrain, to an elevation of 3424 meters above mean sea level. It is one in a series of 15 andesitic stratocone volcanos in the Cascade Range stretching from Mount Garibaldi, British Columbia, in the north to Lassen Peak, California, in the south.

Mount Hood has been chosen by the United States Geological Survey (USGS) as an area for studying the geothermal potential of these Cascade volcanos and as such has been the site of intensive geologic, geochemical, and geophysical investigations. This geophysical investigation was based on an aeromagnetic survey flown in May 1977 by a private contractor for the USGS.

The main goals of this study are: first, to gain a better understanding of the geologic structure of Mount Hood and the surrounding survey area; and second, to assist in locating potential geothermal drill sites.

The geologic units in the area consist mainly of Cenozoic extrusive volcanics whose high remnant magnetizations, combined with the region's high topographic relief, account for most of the short-wavelength, high-amplitude anomalies

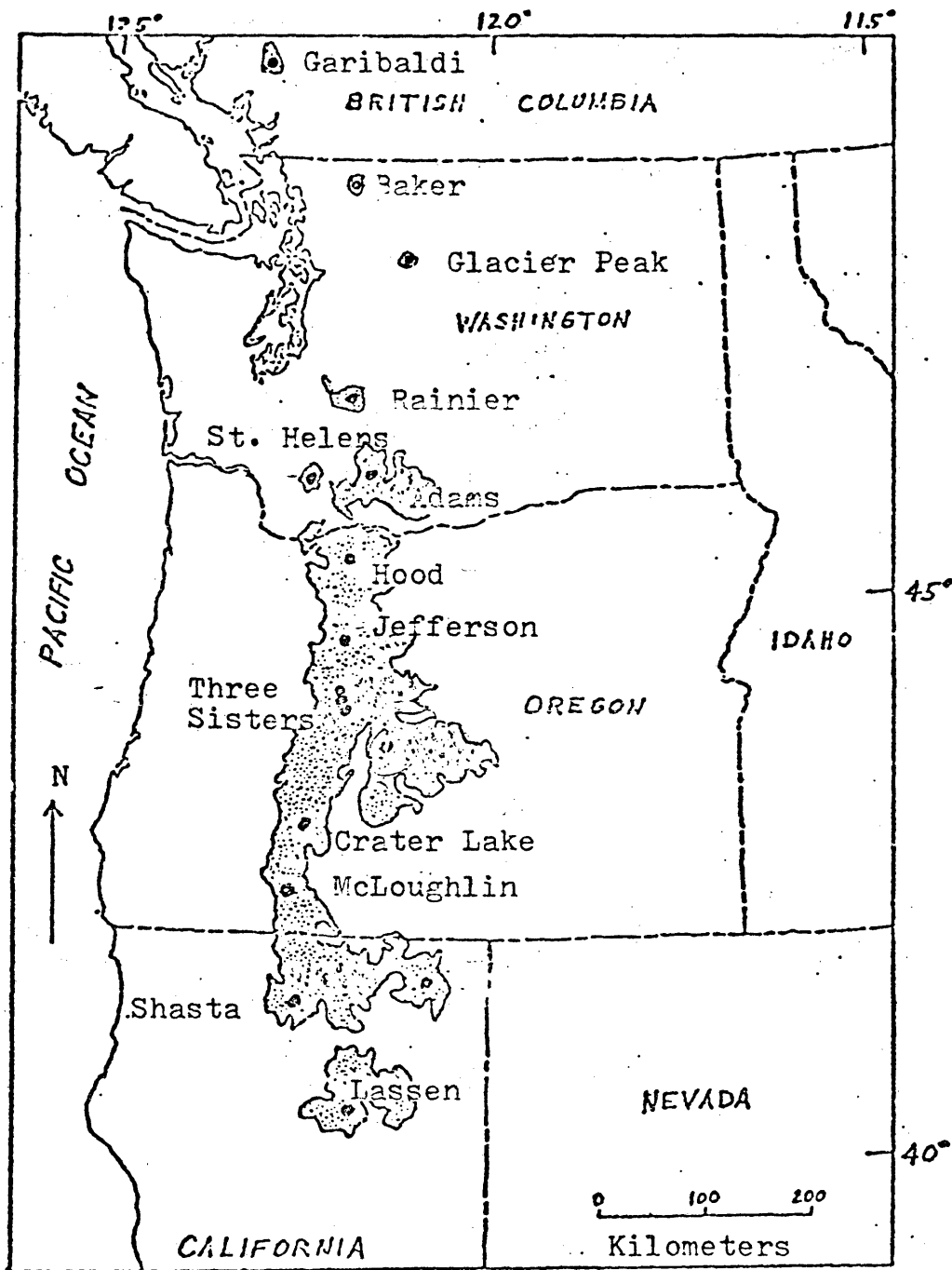


Figure 1. Index map of the Cascade andesitic stratocone volcanos (Blakely and Christensen, 1978).

which are evident on the magnetic contour maps. To better identify the relationships between topography, geology, and magnetic anomalies two studies were undertaken. First, the data was filtered to produce 'upward continued' and 'reduced-to-the-pole' magnetic contour maps of the area. Second, field work was done which consisted of polarity measurements and collection of rock samples in the field. The collected samples were analyzed in the lab for magnetic susceptibility and remnant magnetization.

In the next phase of the investigation a magnetic model was constructed for the Mount Hood volcanic cone using Plouff's (1975) adaptation of Talwani's (1965) three-dimensional modeling program. Initially, a best-fit magnetization vector was found for the entire mountain by a least-squares comparison between the observed magnetic anomaly and the dimensionless calculated anomaly. The determination of the best-fit vector was based on the assumptions that the direction and the intensity of magnetization of the mountain is constant. The least-squares fit yields a residual based on the comparison of the observed field and a field resulting from the mountain being magnetized with the intensity and direction of the calculated best-fit magnetization vector. The residual was used as a basis for constructing a series of magnetic models of the

mountain using a combination of the forward and inverse least-squares calculation routines. The development of the refined magnetic models was controlled by the results of the laboratory analyses on rock specimens from the mountain and by the geologic analysis of Wise (1969).

This thesis uses International System (SI) units. The relation between units in the cgs and SI systems are: for magnetization, $1.0 \text{ emu/cm}^3 = 1000 \text{ amperes/meter (A/m)}$; for susceptibility, $1.0 \text{ emu} = 1/4\pi \text{ SI units (dimensionless)}$; and for magnetic field strength, $1.0 \text{ gamma} = 1.0 \text{ nanotesla (nT)}$.

GEOLOGY

Mount Hood is a recent volcanic cone chiefly composed of andesitic lavas, interlayered with andesitic pyroclastic material. The mountain and surrounding area are underlain by the Yakima Basalt, the volcanoclastic and epiclastic debris of the Dalles and Rhododendron Formations, and the lavas from various Pliocene vents (Wise, 1977).

Except where otherwise cited, the following geologic descriptions are a summary of Wise's study (1969, 38 p., Plate 1).

Late Miocene Deposits

There are two basic types of Late Miocene deposits in the region: basalts, which probably underlie the entire area and clastic debris, which overlies the basalt in the southwest and northeast.

Yakima Basalt

The Yakima Basalt, which is the study area's representative formation of the Columbia River Group basalt flows, is regarded as Middle to Late Miocene in age. It is a low-alumina, high-iron basalt containing little or no olivine and moderate amounts of glass.

Two possibilities for the distribution of the Yakima

Basalt in the Mount Hood area have been suggested. Wise reports that he finds nothing to refute the suggestion that the entire study area is underlain by the Yakima Basalt. However, others have suggested that the area directly beneath Mount Hood was never covered by the basalt as it may have been an area of high topographic relief at the time of emplacement of the Yakima Basalt. This second possibility seems unlikely in light of recent drilling, during which the Yakima Basalt has been encountered, at Old Maid Flats west of Mount Hood.

Rhododendron Formation

The Rhododendron Formation, which overlies the Yakima Basalt in the southwest part of the survey area, is a sequence of conglomerates and agglomerates with interbedded andesite flows. The Rhododendron Formation reaches its greatest known thickness of 430 meters at Zigzag Mountain west of Mount Hood. It thins to the south near the Salmon River Canyon, to the north near Bull Run Canyon, to the east near Barlow Creek, and probably under Mount Hood (Wise, 1977).

The Rhododendron Formation of Upper Miocene or Lower Pliocene age can be petrologically divided into two main occurrences. First, there are unaltered andesitic lava flows which occur near the top of the section at Zigzag

Mountain. Second, there is the volcanoclastic debris which comprises the bulk of the formation. About a third of the volcanoclastic debris is epiclastic mudstones, sandstones, and conglomerates. Another third is pyroclastic tuffs, lapillistones and tuff-breccias. The final third is gradational between the conglomerates and mudflow-breccias.

Dalles Formation

In the northeast, the Yakima Basalt is overlain by the conglomerates, breccias, and interbedded flows of the Dalles Formation, which is contemporaneous with the Rhododendron Formation to the southwest. The Dalles Formation reaches its greatest known thickness of 370 meters east of the Hood River Valley and thins to the south under Lookout Mountain, to the west in the valley of the West Fork of the Hood River and probably under Mount Hood (Wise, 1977).

The Dalles Formation is predominantly epiclastic volcanic boulder-conglomerates and sandstones. However, the formation also contains several layers of unstratified tuff-breccias similar to those found in the Rhododendron Formation. Two flows of hornblende andesite and pyroxene andesite occur near the top of the formation.

Pliocene Deposits

Approximately 210 cubic kilometers of Early Pliocene deposits overlie the survey area. These deposits consist of pyroxene andesites with some intermixed olivine basalts, tuffs, and breccias. At least one granitic intrusion of Early Pliocene age outcrops in the southwest.

During the Late Pliocene as much as 42 cubic kilometers of lava was erupted to the southeast and west of Mount Hood. These lavas range from olivine basalt to hornblende dacite, but are about 80 percent andesite.

In the northeast, at the southern end of the Hood River Valley there are several Early Pliocene deposits of pyroxene andesite. The flows which make up these deposits came from a volcano of which Shellrock Mountain remains as a plug. These lavas which contain some interbedded breccias may also underlie much of the northeast flank of Mount Hood.

North of Mount Hood, in the vicinity of Blue Ridge the Dalles Formation is overlain by olivine basalt lavas of Early Pliocene age. These lavas are in turn overlain by seemingly unrelated andesites of Early to Middle Pliocene age.

A major volcanic center near the present site of Barlow Ridge deposited interbedded flows, breccias, and

dikes of andesite over a large portion of the survey area south of Mount Hood. These Early Pliocene andesites make up Barlow Ridge in its entirety and underlie the area extending from the Salmon River on the west to Bonney Butte on the east and at least as far north as Bennett Pass.

An estimated 34 to 42 cubic kilometers of lava erupted from this volcanic center. Approximately 10 percent of the flows are basalts. The remainder of the lavas are pyroxene andesites with a few hornblende dacites. All of the flows and breccias outcropping in the area exhibit some alteration.

Badger Butte, to the southeast of Mount Hood, is located at the center of a series of Late Pliocene flows that are exposed in the surrounding canyons. Similar exposures are found on the flanks of Bonney Butte, Lookout Mountain, Bluegrass Ridge and the east flank of Mount Hood. The flows sequentially consist of olivine andesites at the lowest exposure north of Badger Lake to andesites containing less olivine and more pyroxene at the highest exposure near Bonney Butte.

The sequence near Gunsight Butte is overlain by flows which emerged from near Bonney Butte. These flows, which form the top of the ridge from Badger Butte northward for several kilometers are composed of olivine basalts and

olivine andesites.

Two Early Pliocene intrusions are exposed southwest of Mount Hood. The Laurel Hill Intrusion outcrops in a small area centered at Laurel Hill just to the north of Tom Dick Mountain. The Still Creek Intrusion outcrops along the base of the Still Creek Valley on the south flank of Tom Dick Mountain.

Both intrusions are porphyritic quartz diorite to quartz monzonite. There is evidence to suggest that the intrusions are linked to a single, larger pluton of which these exposures are only the eroded upper sections.

Tom Dick Mountain is capped by olivine andesite and pyroxene andesite flows of Late Pliocene age. These flows lie over metamorphosed tuffs and lavas and possibly on the Still Creek Intrusive. The andesite flows are up to 300 meters thick and seem to be genetically related to the lavas on the west side of Mud Creek Ridge.

On Zigzag Mountain, west of Mount Hood, the Rhododendron Formation is overlain by 760 meters of Early Pliocene pyroxene andesites and interflow tuffs. The approximately 100 cubic kilometers of andesites can be traced discontinuously from the north side of Lost Lake south to Tom Dick Mountain. The flows seem to have originated from five stocks; three on the south slope of Zigzag Mountain

and two along the Sandy River Canyon to the north.

On the top of Zigzag Mountain, the pyroxene andesites are overlain by approximately 100 meters of Late Pliocene olivine basalt flows with interbedded tuffaceous debris. One large andesite flow originated from a vent on the eastern end of the mountain and flowed southwest down an old canyon-cut into the olivine basalts.

A string of Late Pliocene, olivine basalt and olivine andesite flows stretch from the northwest corner of Mount Hood, northwest past Bull Run Lake. The flows, which account for 6.3 cubic kilometers of lava, generally form a series about 250 meters thick. Individual flows such as the olivine andesite that underlies Hiyu Mountain are as much as 90 meters thick.

The base of the Sandy Glacier, on the western flank of Mount Hood, is the scene of a series of steep exposures of flows and tuffs. Flows less than three meters thick alternate with tuffs and agglomeritic breccias overlying the lowest flows of altered olivine basalt. The total thickness is over 900 meters and the flows are interpreted as the remains of a large Late Pliocene volcano that first erupted olivine basalt, then pyroxene andesite.

Quaternary Deposits

The most extensive Quaternary deposits are those that comprise the bulk of the Mount Hood volcano. However, many of the other landforms, although affected by Fraser Glaciation (15000 years before present), are the result of Quaternary volcanos and flows. The Quaternary flows range from olivine basalt to pyroxene andesite and hornblende dacite.

Outlying Deposits

Northeast of Mount Hood at the edge of the survey area are two large domes known as the Mill Creek Buttes. The flows that originated from the domes are 150 to 250 meters thick and cover the area between the buttes and the present site of the East Fork of the Hood River. Large amounts of hornblende-bearing pumice is found both underlying and between the flows which are composed of hornblende dacite.

From the south flank of Lookout Mountain, to Grasshopper Point, the ridges and mountains are capped by a series of related flows. The flows, which are as much as 15 meters thick, are composed of olivine basalt and olivine andesite. The vents from which the flows originated are easily located as red, remnant cinder cones.

A series of flows comprising about 1.3 cubic kilometers of lava originated along the top of Blue Ridge north

of Mount Hood. The flows, which emerged from at least eight separate vents, are composed of olivine basalt, olivine andesite and aphanitic andesite.

Lost Lake Butte is a large volcanic butte located northeast of Lost Lake at the edge of the survey area. The flows from this butte were olivine andesite and contributed a volume of 31.5 cubic kilometers of lava. The last flow cut across a gap in Butcher Knife Ridge and flowed east into the valley of the West Fork of the Hood River.

South of Lost Lake and a few kilometers west of Lolo Pass there are three small patches of hornblende andesite. These andesites are the remnants of flows originating from two plugs that have been uncovered by a tributary of Clear Fork.

Mount Hood Volcano

The Mount Hood volcano, located in the center of the survey area is composed of nearly 190 cubic kilometers of flows and pyroclastic debris. Debris eroded from the cone is found in all of the valleys draining from the mountain and is chiefly due to the erosion of the Fraser Glaciation period.

The Mount Hood volcanic cone can be divided into four major units. The first unit which accounts for the bulk of the volcano is marked by two distinctive types of

deposits. The first type of deposit is long intracanyon flows of pyroxene andesite, 10-13 kilometers in length, which comprise most of the volcano below 2400 meters elevation. Single flows of this type were as large as 2.1 cubic kilometers and filled canyons radiating from the mountain to depths of 150 to 180 meters. The projection of these flows back toward the center of the mountain indicate that they are the result of the volcano while its vent was still at or below 2450 meters elevation. The second type of deposit consists of thin pyroxene andesite flows and interbedded clastic debris and comprises the upper portion of the mountain. These deposits were mostly small flows that spread out over the steep sides of the cone as it grew from an elevation of 2400 meters to almost 3660 meters. However, there are at least two thick flows originating from vents well over 2400 meters in elevation.

The second unit consists of olivine andesite erupted from satellite cones. These satellite cones, The Pinnacle, on the north slope, and Cloud Cap, on the northeast slope of the mountain are sources of pre-glacial olivine andesite flows that are in excess of 15000 years old (White, 1978).

The third unit consists of a large hornblende-dacite plug-dome, near the summit of the mountain, and its associated pyroclastic debris which litters the southwest slope

of the volcano. This plug-dome, of which Crater Rock remains as a remnant, was extruded following a long period of little activity during which the volcano was glaciated.

The fourth and final unit consists of debris from several dacite block and ash flows which occurred over the last two thousand years. The Timberline flow which came down the south slope of the mountain (1700 years before present) and the Old Maid Flat flow (200-250 years before present) are two documented flows (White, 1978). However, there may have been other eruptions as recently as the late 1800's.

THE AEROMAGNETIC DATA

The aeromagnetic survey covers an area (Plate 1a) of approximately 1750 square kilometers between 45°11' and 45°34' north latitude and 121°23' and 122°00' west longitude. The survey was flown in two parts. The first part (low-level), flown at about 2134 meters barometric elevation, covers the flanks of the mountain and surrounding areas (Fig. 2, Plate 2). The second part (high-level), flown at about 4267 meters barometric elevation, covers an area of approximately 228 square kilometers centered over the peak of the mountain (Fig. 3, Plate 3). The survey was flown east-west at approximately one-mile line spacings. Two tie-lines, one east and one west of the mountain, were flown north-south at 2134 meters elevation.

Data Processing

The contractor prepared the total-field flight-line file from the raw digitized flight-line data by:

1. editing obvious random errors,
2. removing temporal variations of the magnetic field based on a continuously monitored ground magnetometer,
3. correlating the flight-lines with topographic maps via air photos,

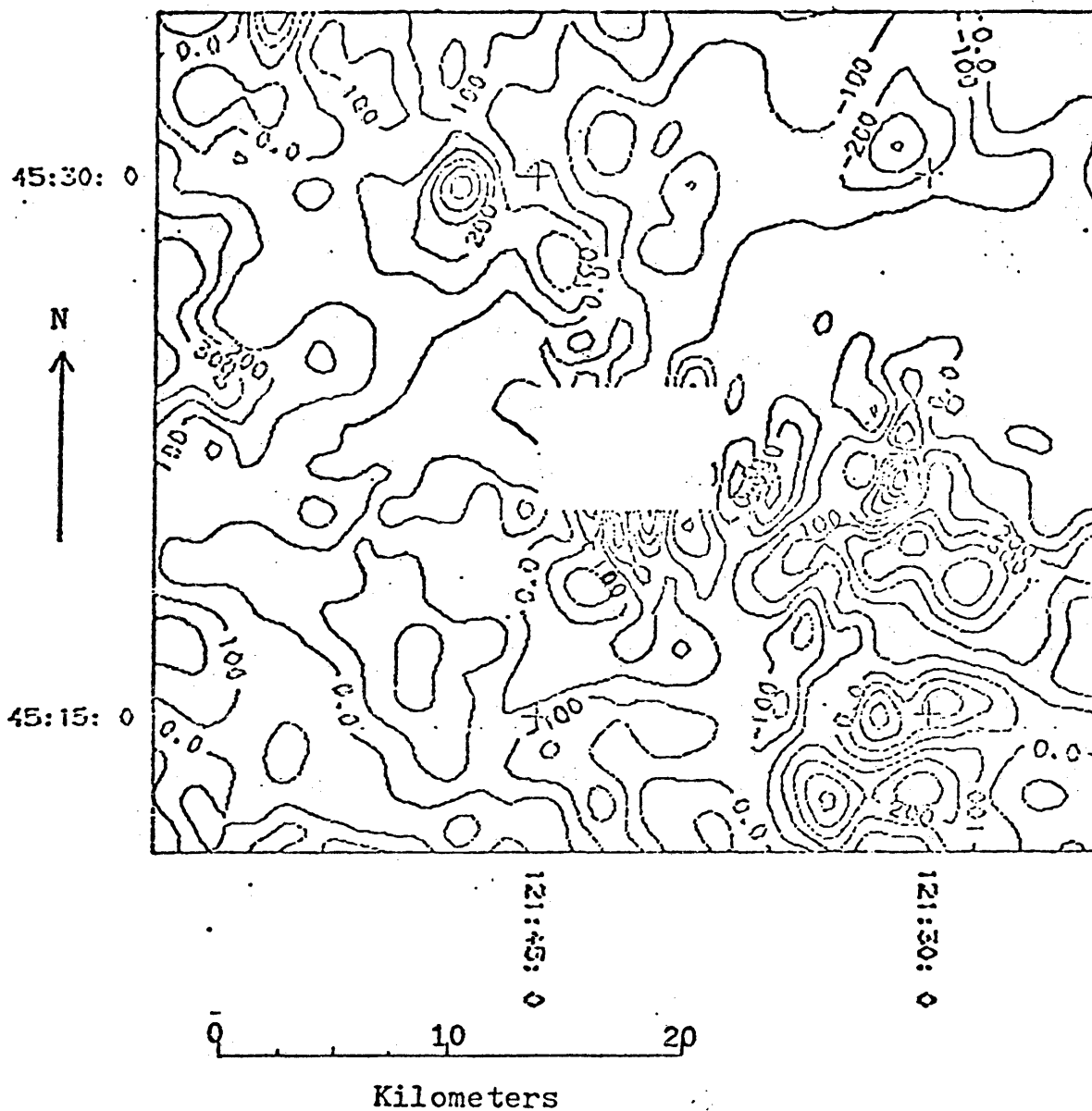


Figure 2. The low-level aeromagnetic survey of the flanks of Mount Hood and the surrounding area.

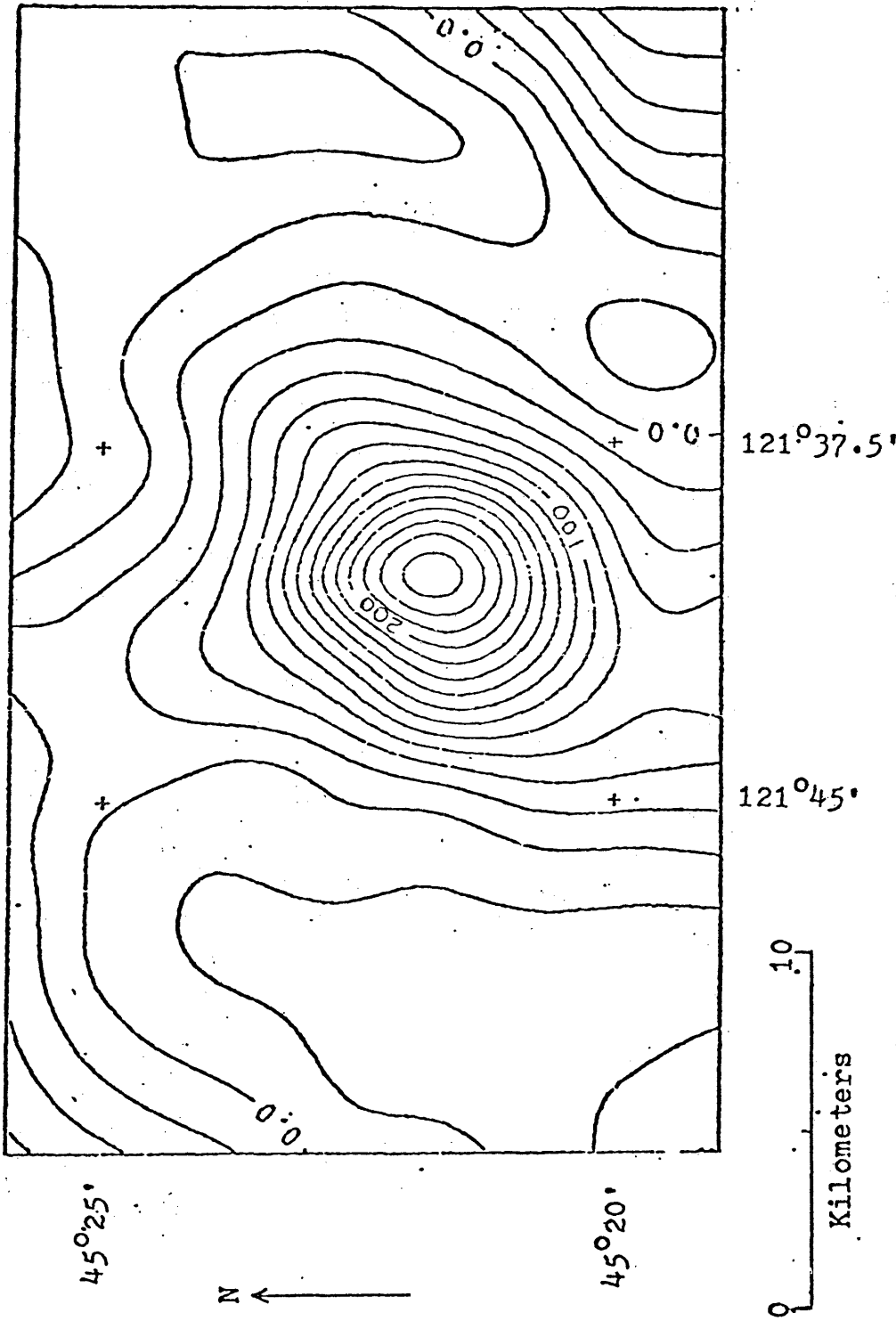


Figure 3. The high-level aeromagnetic survey of the Mount Hood volcanic cone.

and 4. adjusting flight-lines and tie-lines to agree.

The total-field flight-line file was then prepared for creating contour maps for analysis by:

1. gridding the total-field magnetic values, by minimum curvature methods, onto an evenly spaced, 0.8 kilometer grid,
- and 2. removing a quadratic approximation of the International Geomagnetic Reference Field (IGRF), updated to June 1977.

It should be noted that the data file resulting from the above processing was used only for producing contour maps for a qualitative analysis of the study area and not as input to the modeling routine. The input data for the modeling program need not be gridded, and therefore, the contractor's flight-line file was processed differently for input to the modeling routine (see Modeling Program Input, page 44).

Transformations of the Aeromagnetic Data

To further the qualitative analysis of the data a number of transformations were performed on both the high- and low-level data sets. One such transformation was the upward continuation of the low-level data set to the same elevation as the high-level data set. The upward continued low-level data was then integrated with the high-level data

to create a continuous data set at an elevation of 4267 meters. Finally both the low-level and integrated data sets were reduced-to-the-pole.

Upward Continuation

To eliminate the effects of near-surface, high-amplitude and short-wavelength anomalies and to assist in the production of an integrated aeromagnetic map the low-level survey data was upward continued to an elevation of 4267 meters using the USGS program "CONVER" (Hildebrand, 1978). "CONVER" employs the use of the discrete, Fourier transform method discussed by Fuller (1967) and Lourenco (1972). Initially, the space-domain, two-dimensional gridded data set is transformed into the frequency domain via the fast Fourier transform. The resulting Fourier spectrum is then multiplied by the coefficients of the appropriate digital filter (in this case the upward continuation coefficients). Lastly, the product of the filter response and data spectrum is inversely transformed to obtain a filtered map in the space domain.

The upward continued map (Fig. 4, Plate 4) that results from this transformation is a representation of how the aeromagnetics over the survey area would appear if measured at an elevation of 4267 meters.

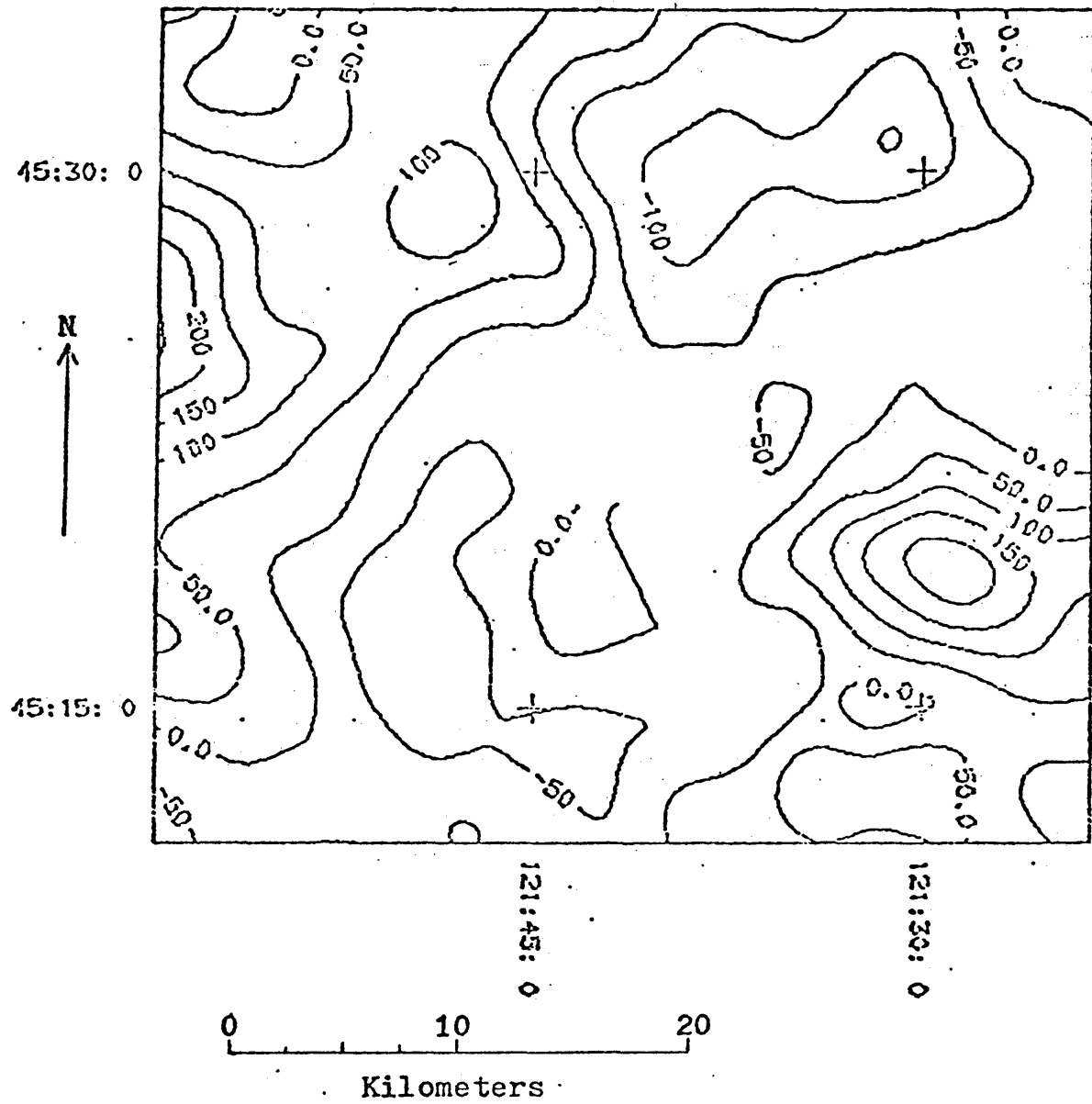


Figure 4. The upward continued version of the low-level aeromagnetic survey.

Integration

Following the upward continuation of the low-level aeromagnetic survey the upward continued data was combined with the high-level data into a single complete map (Fig. 5, Plate 5) at an elevation of 4267 meters above mean sea level. The process of combining the two data sets is referred to as integration.

Before performing the integration, the upward continued data near the hole due to the missing low-level data, was visually compared to the overlap of the high-level data to check on agreement between the two data sets. A constant 20 nT was added to the low-level upward continued data based on the inspection.

To perform the integration, the two original data sets must be gridded on the same grid lines and projected with the same base-latitude and central meridian. A second qualification is that the data set to be inserted has the same dimensions as the hole in which it is to be inserted. Thus, the border of the high-level data set was removed to reduce it to the same size as the hole in the upward continued data.

The data sets are then combined and the resulting integrated map is contoured and inspected to determine if smoothing is required along the border of the inserted data. In the present case smoothing was required along the southern

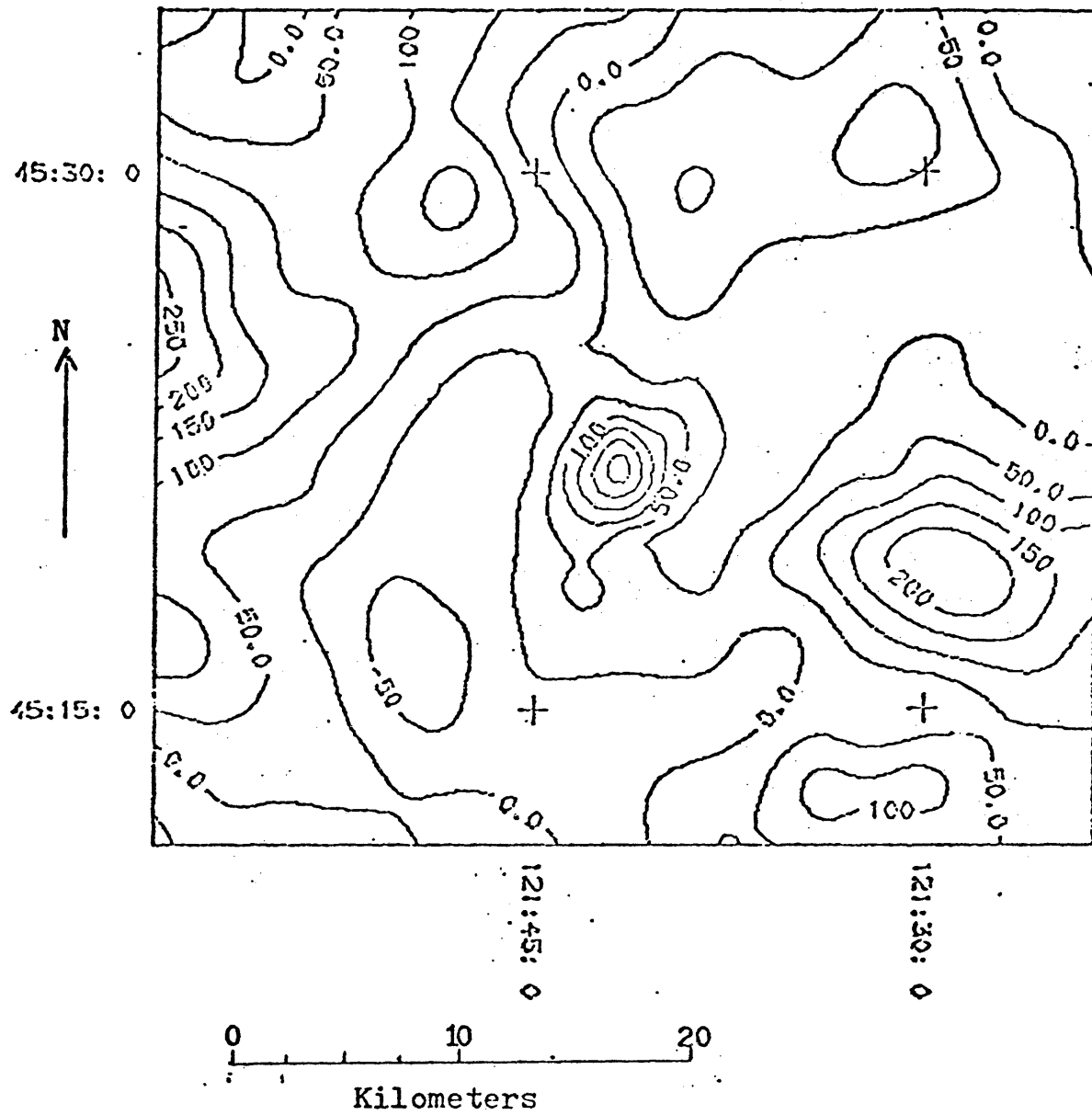


Figure 5. The integrated version of the Mount Hood aeromagnetics.

edge of the inserted data. Since the high-level data is real and the low-level data is the result of the upward continuation operator two rows of points were removed from the upward continued data along the south edge of the inserted high-level data. The hole created by the removal of these points was then smoothed over by creating new grid points, based on the surrounding data, using the minimum curvature gridding routine (Webring, 1978). The smoothed grid was then contoured to produce the final integrated map (Fig. 5, Plate 5).

Reduction-to-the-Pole

To better identify the causative bodies of the various magnetic anomalies the low-level and integrated high-level aeromagnetic data sets were reduced-to-the-pole via "CONVER" (Fig. 6 and 7, Plates 6 and 7). The purpose of this transformation is to reduce the effects due to non-vertical rock-polarity and magnetic field vectors. The effect of non-vertical magnetic vectors, on the anomaly resulting from a magnetized body, is to distort the size, shape, and position of the anomaly and thus, make interpretation more difficult.

Reduction-to-the-pole (Lourenco, 1972) is a mathematical technique to transform the observed magnetic anomaly values into the values that would be observed if the same body was located at the magnetic pole and had a vertical magnetization

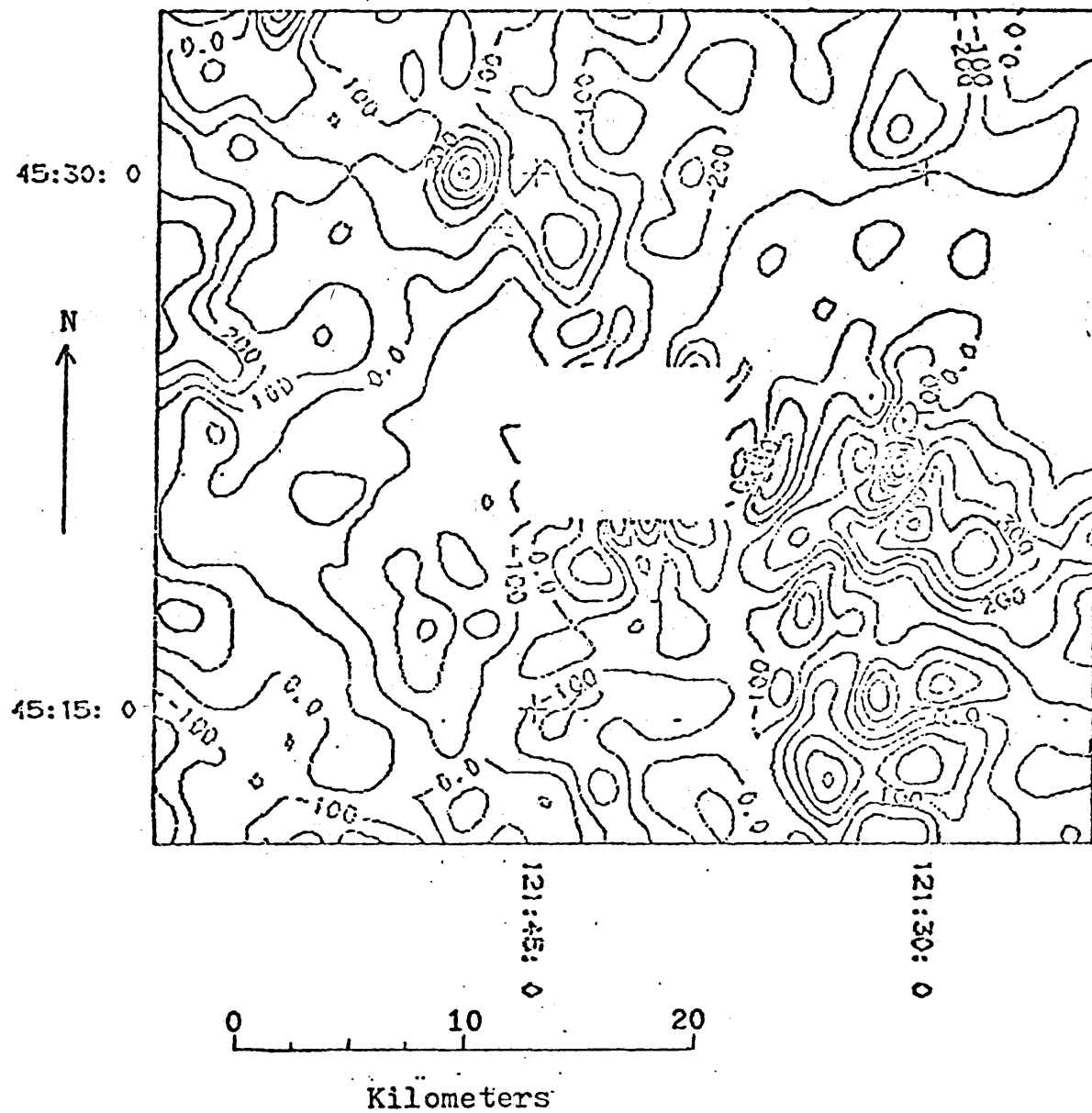


Figure 6. The reduced-to-the-pole version of the low-level aeromagnetic survey.

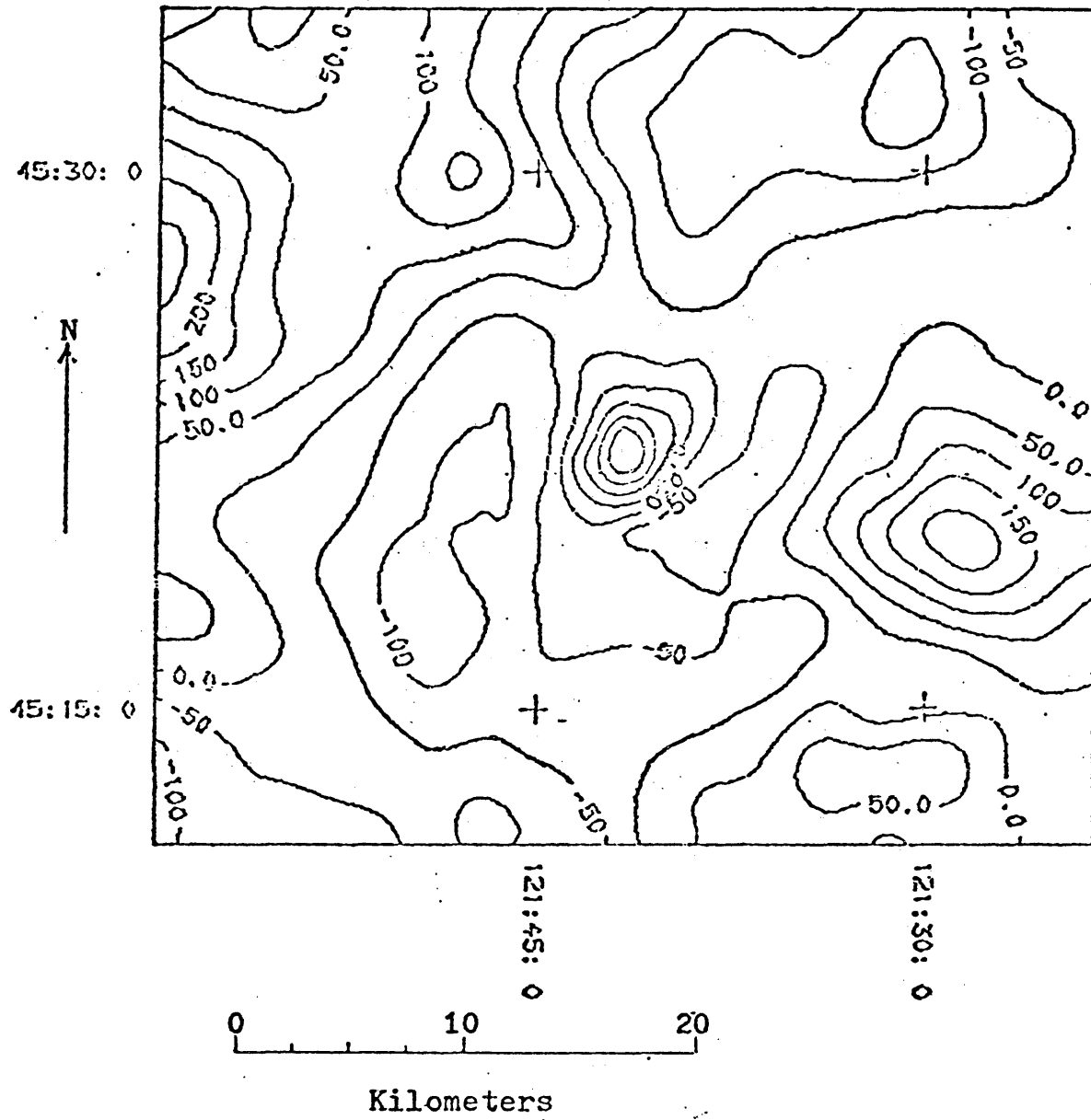


Figure 7. The reduced-to-the-pole version of the integrated Mount Hood aeromagnetics.

vector. Theoretically, a symmetrical body would, following reduction-to-the-pole, exhibit a symmetrical anomaly centered over the centroid of the body as in the gravity case.

Although this process may give us further insight into the location and extent of various anomalies it cannot be relied upon exclusively since intrinsic to the theory is the assumption that all of the bodies in the area to be reduced have directionally identical magnetization vectors.

In the case of the Mount Hood aeromagnetics, laboratory and field polarity results indicate that a large percentage of the rocks have polarity vectors either close to the direction of the Earth's field or directly opposed to the direction of the Earth's field. Thus, the reduction-to-the-pole was done using the assumption that the entire area has magnetization vectors which are in the direction of the Earth's present field. The effect of the assigning of a normal polarity vector to the entire area has on the reversed polarity outcrops is that they appear as if they had a -90° inclination rather than the 90° inclination that would result from true reduction-to-the-pole. Our results are thus more advantageous for interpretation since all the anomalies are now located over the causative bodies and the anomalies resulting from the reversed polarity rocks are magnetic lows.

LABORATORY AND FIELD WORK

To assist in the qualitative analysis of the low-level aeromagnetics and to establish additional constraints on the quantitative modeling of the Mount Hood cone anomaly, rock samples were collected for laboratory studies of magnetic susceptibility and natural remnant magnetization (NRM). Field polarity measurements were made on 30 samples. Laboratory studies to determine NRM and susceptibility were done on 70 samples including 47 for which no field polarity was found.

Measurement of Remnant Magnetization and Susceptibility

Measurements to determine the NRM were made using a Schonstedt model SSM-1A spinner magnetometer. Each core was spun twice in three-orthogonal directions and the results averaged to obtain the magnitude of the magnetic moment. The total magnetization vector was found for cases in which the cores were oriented.

Demagnetization experiments to eliminate the effects of low-relaxation time remnance, such as that due to lightning strikes, were done using a Schonstedt model GSD-1 AC-demagnetizer. In all the experiments the demagnetizing field decay rate was set at 5000 nT (50 millioersteds) per

half cycle. The field was varied between 10 and 60 milliteslas (100 and 600 oersteds). After each demagnetization the core was again spun on the spinner magnetometer and the magnetization vector compared to the previous results. The process was repeated until a stable direction was obtained.

The susceptibility of each of the 70 samples was determined using a Bison model 3101A susceptibility bridge.

Analysis of Results

The results of the laboratory measurements were analyzed statistically. Average values for susceptibility and remnance were found and when appropriate the standard error of the mean is stated. The standard error of the mean (s) is found from:

$$s = \sqrt{\frac{\sum x_i^2 - \frac{(\sum x_i)^2}{n}}{n-1}}$$

where x_i is the i th measured value,

and n is the number of measurements.

The laboratory analysis of magnetization and susceptibility indicated a number of significant variations in the magnetic properties of the rocks comprising Mount Hood and the surrounding area. The results of 20 samples of Mount

Hood andesites, both flows and pyroclastics, analyzed for susceptibility and remnant magnetization are found in Table 1. Excepting 3 samples (18, 43 and 62) which showed unusually high values of remnant magnetization the average susceptibility (k) was $1.7 \times 10^{-2} \pm 0.7 \times 10^{-2}$ SI units and the average remnant magnetization (J_r) was 2.1 ± 1.1 A/m. These values are comparable to those at Mount Shasta where the average remnant magnetization was found to be 2.0 A/m (Blakely and Christian- sen, 1978).

Two distinct areas of the Mount Hood cone have magnetic properties which are not in agreement with the general characteristics indicated above. An analysis of 4 samples from the crater area near the summit of the mountain (Table 2) indicates an average remnant magnetization of 13.66 ± 8.6 A/m and a Koenigsberger (Q) ratio of 32.4.

At least two points should be made in regard to the crater area rocks. First, these rocks which exhibit the highest remnant magnetizations in the survey area may be dacites. Second, they are almost certainly magnetized in the direction of the Earth's present magnetic field since the crater area represents the late stage outpourings of the volcano.

The second area of disagreement is the Sandy Glacier

TABLE 1

Laboratory Results on Mount Hood Andesites

Sample	Location	k x 10 ⁻²	Jr	I	D	Q
18	Timberline	0.79	7.26	-	-	21.4
19	Timberline	1.75	2.08	83.2	-71.5	2.8
21	Timberline	1.78	1.55	64.6	170.0	2.0
38	Cloud Cap	2.01	2.87	70.8	4.6	3.3
40	Cloud Cap	3.12	1.55	63.9	8.1	1.2
41	Cloud Cap	2.01	1.27	-	-	1.5
43	Cloud Cap	0.35	7.74	-	-	51.2
45	Cloud Cap	0.50	0.94	53.9	-2.1	4.4
46	Cloud Cap	1.36	4.01	78.0	-33.3	6.8
47	Cathedral Ridge	1.76	1.67	-	-	2.2
49	Cathedral Ridge	1.23	3.75	-	-	7.1
50	Mississippi Head	2.31	2.21	-	-	2.2
51	Barrett Spur	1.83	3.25	-	-	4.1
61a	Hood Meadows	2.07	0.60	-	-	0.7
61b	Hood Meadows	0.34	1.08	-	-	7.3
62	Hood Meadows	1.43	18.30	-	-	29.8
64	Hood Meadows	1.89	4.28	-	-	5.3
65	Hood Meadows	1.85	1.22	-	-	1.5
67	Hood Meadows	1.53	1.74	61.4	3.4	2.6
68	Hood Meadows	0.92	1.46	52.3	6.0	3.7
Avg. w/o 18, 43, 62		1.66	2.09			2.9

TABLE 2

Laboratory Results on Crater Area Rocks

Sample	Location	$k \times 10^{-2}$	Jr	I	D	Q
102	Crater Area	1.59	22.76	-	-	33.3
103	Crater Area	1.04	19.29	-	-	43.0
105	Crater Area	0.29	6.74	-	-	54.3
106	Crater Area	1.00	5.84	-	-	13.7
Average		0.98	13.66			32.4

Volcano which is exposed on the northwest flank of Mount Hood. An analysis of 6 samples (excluding sample E) from this area (Table 3) show an average remnant magnetization of 0.42 ± 0.14 A/m and a Q ratio of 0.5. Of even more importance is that these 6 samples have magnetization directions which indicate that part of this volcano is reversely magnetized. Therefore, the total magnetization cannot be found without taking into account the directions of magnetization. If these rocks were all normally magnetized in the direction of the Earth's field the value of the total magnetization would be 1.3 A/m, which is still well below the average for the Mount Hood andesites. However, if the entire volcano were reversely magnetized the value would be 0.48 A/m. The actual value probably lies somewhere between these two values.

TABLE 3

Laboratory Results on the Sandy Glacier Volcano

Sample	$k \times 10^{-2}$	Jr	I	D	Q
A	1.88	0.52	-	-	0.6
B	2.12	0.58	37.4	-155.8	0.6
D	2.33	0.45	77.9	-22.1	0.5
E	2.13	5.40	69.2	20.5	5.9
F	2.27	0.19	-75.2	94.9	0.2
G	1.62	0.42	-18.1	-164.4	0.6
H	2.39	0.34	-40.6	-159.6	0.3
Avg. w/o E	2.10	0.42			0.5

Another area which yielded interesting laboratory results was east of Mount Hood near Dog River Springs (Table 4). The average susceptibility of $0.20 \times 10^{-2} \pm 0.15 \times 10^{-2}$ SI units for the 3 samples from this area was the lowest in the survey area. The average remnant magnetization of 2.9 ± 2.8 A/m yielded an average Q ratio of 34.4. The total magnetization would be 3.0 A/m if the rocks are normally magnetized but more important (upon examination of the aeromagnetic contour map, Figure 2) the total magnetization could be as much as 2.8 A/m in the direction opposite to the Earth's field if the rocks are reversely magnetized. Since no outcrops could be found in the area the analysis was based on float and thus, there

was no opportunity to ascertain the remnant direction.

TABLE 4

Laboratory Results on Basalts from Dog River Springs

Sample	$k \times 10^{-2}$	Jr	I	D	Q
25	0.37	6.10	-	-	38.4
52	0.12	1.12	-	-	22.6
53	0.10	1.46	-	-	33.0
Average	0.20	2.89			34.4

The results of laboratory measurements on samples from other localities are found in Table 5. Where appropriate these results are referred to in the next section on qualitative analysis. However, only one or two samples per locality and a lack of information on the directions of magnetizations restrict the ability to draw firm conclusions from this data.

It should be noted that the laboratory results are based solely on surface outcrops and float and as such may not represent the bulk properties of the rocks comprising the mountain or surrounding areas.

TABLE 5

Laboratory Results on Rock Samples

Sample	Location	k x 10 ⁻²	Jr	I	D	Q
2	Laurel Hill	2.75	0.73	-	-	0.6
3	Still Creek	3.81	0.21	-49.3	21.7	-
4	Still Creek	0.09	0.025	-	-	0.6
5	Tom Dick Mountain	2.07	0.95	-	-	1.1
7	Tom Dick Mountain	1.82	0.32	-	-	0.4
8	Tom Dick Mountain	0.71	0.50	-	-	1.6
9	Lost Lake Butte	0.12	3.81	-	-	7.3
10	Lost Lake Butte	1.69	3.46	-	-	4.8
12	Red Hill	2.02	4.27	-	-	4.9
13	Red Hill	0.96	0.83	-	-	2.0
14	Bear Creek	1.02	4.96	-	-	11.3
15	Bear Creek	1.77	1.21	72.3	-82.5	1.6
16	Cooper Spur	1.32	1.05	64.3	33.5	1.9
17	Cooper Spur	1.36	2.11	-	-	3.6
22	Windy Fork	1.71	1.94	70.6	-3.5	2.6
23	Windy Fork	2.50	1.56	-40.0	165.9	1.5
27	Robinhood	4.93	1.93	-	-	0.9
29	Mill Creek Buttes	0.29	1.29	-	-	10.4
30	Mill Creek Buttes	0.70	0.16	-50.2	-167.4	0.7
31	Mill Creek Buttes	0.97	0.10	-	-	0.2
32	Zigzag Mountain	1.69	2.02	69.3	14.4	2.8

TABLE 5 (cont.)

Sample	Location	k x 10 ⁻²	Jr	I	D	Q
33	Zigzag Mountain	2.22	1.98	74.6	15.5	2.1
34	Grasshopper Pt.	1.08	11.82	-	-	25.5
42	Cooper Spur	2.06	1.69	-	-	1.9
55	Bonney Butte	1.38	5.85	-	-	9.8
56	Bonney Butte	1.43	7.76	-	-	12.6
57	Cloud Cap	1.87	3.22	73.5	-9.5	4.0
58	Cloud Cap	1.16	0.76	-	-	1.5
59	Cloud Cap	1.24	1.34	-	-	2.5
60	Cloud Cap	0.51	10.06	-	-	45.9
69	Pinnacle	0.68	1.70	52.0	3.0	5.8
71	Pinnacle	2.05	23.69	44.3	127.8	26.9
72	Red Hill	2.19	1.27	72.1	-48.3	1.4
35	Bluegrass Ridge	1.33	0.96	9.4	-138.3	-
36	Bluegrass Ridge	1.61	0.15	-60.4	-169.8	0.2
37	Bluegrass Ridge	2.63	0.97	53.8	-175.1	-

QUALITATIVE ANALYSIS

Many of the anomalies seen on the aeromagnetic maps are associated with, and may be in a large part due to, topographic and surface geologic features. One of the main reasons for producing reduced-to-the-pole and upward continued contour maps from the original data was to make evident these relationships between the magnetic anomalies, topography, and geology.

This qualitative analysis was accomplished by a comparison of the various magnetic maps, Wise's (1969) discussion and geologic map, and the topographic maps of the region. Further assistance was obtained from the results of field observations of magnetic polarities and laboratory analyses of the remnant magnetization and magnetic susceptibility.

For the most part the results contained herein are the most obvious and the least complicated explanations. However, without more extensive field observations and considering the non-unique nature of potential fields a more complex analysis is not warranted and is beyond the scope of this thesis.

Southwest of Mount Hood, at Tom Dick Mountain, there is a magnetic low of -257 nT (Fig. 2, Plate 2).

The magnetic low is probably the result of two factors: first, the mountain is capped by reversely polarized Late Pliocene Volcanics and second, the mountain is underlain by the only known silicic intrusive in the area. Initially it was thought that the low magnetic susceptibility and remnance of the intrusive, with respect to the extrusive basalts and andesites, and its' large size were good explanations for the negative-sign and long-wavelength of the anomaly. However, the few measurements of magnetic properties that are available (Table 5, samples 2 and 3) indicate that the susceptibility is approximately twice as high (3.28×10^{-2} SI units) as the Mount Hood andesites. Therefore to explain the anomaly by a variance in total magnetization from the surrounding rocks the remnant component must be reversed. Although no lab results of the remnant direction are available, reversed polarity is quite possible since the pluton is Early Pliocene in age.

The supposition that the anomaly at Tom Dick Mountain is caused by a body of large dimensions (i.e. the granitic intrusive) is supported by the anomaly's appearance on the upward continued version of the aeromagnetics. Since upward continuation acts as a low-pass filter we would expect that only the larger-scale features would be preserved.

Northwest of Mount Hood, at Lost Lake Butte, a

magnetic high of 601 nT (Fig.2, Plate 2) is most likely the result of the large quantity of normally polarized olivine andesite of which the butte is composed. The extremely high-amplitude anomaly probably is the result of the rocks which comprise this butte having higher remnant magnetization (3.64 A/m versus 2.1 A/m for Mount Hood andesites) than the surrounding volcanics (Table 5, samples 9 and 10).

Magnetic lows of 311 nT, and 240 nT occur east and southeast of Mount Hood over Bluegrass Ridge and Gunsight Butte respectively (Fig. 2, Plate 2). These lows can best be explained by the reversely magnetized Late Pliocene Volcanics which cap both Bluegrass Ridge and Gunsight Butte.

The high-amplitude (-617 nT), short-wavelength negative anomaly at Dog River Springs, east of Mount Hood, (Fig. 2, Plate 2) is not easily explained in terms of topography or surface geology. The lack of outcrops in the area forced the use of float as samples for laboratory analysis. The results of this analysis (Table 4) were very distinctive, the samples having very low susceptibilities (0.15×10^{-2} SI units) and high remnance (2.9 A/m). Assuming the remnance is reversed the anomaly is easily explainable due to a near-surface concentration of these types of rocks. These rocks, which are red in color, may

be part of one of the Quaternary vents that Wise (1969) identifies as old, buried red cinder cones between the Dog River Canyon and Grasshopper Point or a buried vent of the same type.

The laboratory results on the one sample collected at Grasshopper Point (Table 5, sample 34) are comparable to those at Dog River Springs. The sample having low susceptibility (1.08×10^{-2} SI units) and high remnance (11.82 A/m). These laboratory results and the magnetic low of -243 nT which occurs over Grasshopper Point indicate that these old Quaternary cones are composed chiefly of rocks with high reversed remnant magnetizations giving rise to high-amplitude, short-wavelength anomalies on the low altitude aeromagnetic map.

North of Mount Hood, near Red Hill and Blue Ridge, the magnetic high of 299 nT (Fig. 2, Plate 2) is probably a result of the normally polarized flows of Early Pliocene Volcanics in the area and the higher than average topography which enhances the affect of these rocks relative to the surrounding rocks.

The series of magnetic lows (-268, -268, -248, -176, and -370 nT) to the north and northeast of Mount Hood (Fig. 2, Plate 2) are to some extent probably due to the low elevations (800 meters and less) of the Hood River

Valley. The general widespread affect of the low elevations can be seen better on the upward continued versions of the aeromagnetic maps. There the various negative anomalies blend into one long-wavelength negative anomaly. Some of the high-frequency anomalies which appear on the low-level versions may be due to local concentrations of reversely magnetized Dalles Formation rocks.

The high-amplitude anomaly of 265 nT in the center of the integrated version of the aeromagnetics (Fig. 5, Plate 5) represents the topographic-magnetic expression of the Mount Hood volcanic cone. The anomaly has an extension to the south (a magnetic high of 242 nT on the low-level map) which is at present unexplained geologically or topographically.

MODELING

Computer methods to calculate the magnetic anomaly resulting from a magnetized three-dimensional body have been expounded since the early 1960's (Vacquier, 1962; Bott, 1963; and Talwani, 1965). Although all of these methods have proved valuable in the interpretation of magnetic anomalies, they have been limited in their accuracy and scope of application. The main limiting factor has been the use of analytical integration in only the x- and y-directions when calculating a body's volume integral, the z-direction integration having been done numerically.

The method used herein was developed by Plouff (1975) as an improvement on the method of Talwani (1965) and applied by Blakely and Christensen (1978) to a similar problem at Mount Shasta, California. Plouff calculates the magnetic field due to a series of polygonal prism bodies by integrating the volume integrals of Talwani (1965) in the z-direction. By doing the z-direction integration analytically Plouff obtained a more accurate representation of the body and thus, an improved representation of the magnetic field due to the body. The value of the average direction and intensity of magnetization for the body can be assumed, calculated from sample data, or a best-fit total magnetiza-

tion determined. The best-fit total magnetization can be found by a least-squares comparison between the observed anomaly and a dimensionless calculated anomaly based on the inputted topographic model.

A geologic-magnetic model of the Mount Hood cone is developed in two main steps. First, a best-fit magnetization vector is found for the entire cone and a residual map generated by subtracting the calculated field from the observed field. Second, the best-fit residual is used as a basis for constructing a more refined model of the Mount Hood cone. The refined model is developed by using the inverse least-squares and forward calculation routines in conjunction with magnetic and geologic data to add inhomogeneities in the mountain's magnetic structure. A series of iterations are done until a satisfactory mathematical, geophysical and geological model is obtained.

Initial Least-Squares Modeling

The high-level anomaly of 265 nT (Fig. 3) resulting from the Mount Hood volcanic cone is dominated by the magnetic expression of the topography. As such it is difficult to make any interpretation as to anomalous magnetic masses within the body of the cone. To reduce this problem a best-fit magnetization vector for the entire cone was calculated using the least-squares technique. The field

calculated from magnetizing the mountain with the best-fit magnetization is subtracted from the observed field to yield a residual. This residual is then an expression of where the assumption of uniform magnetization is incorrect.

The least-squares best-fit magnetization is based on the two simplifying assumptions of uniform direction and intensity of magnetization for the mountain as a whole. Although these two assumptions are an over simplification of the problem there are at least three reasons to believe that they might yield a viable initial magnetic model of the mountain. First, the bulk of the volcano has probably been built in the last 100,000 years (Wise, 1978) and thus, is probably normally magnetized. Second, although the assumption of uniform intensity is not accurate in detail, laboratory results (Table 1) indicate that the assumption is probably reasonable (average magnetization of lab samples was 2.8 ± 1.2 A/m). Third, the observed anomaly (Fig. 3) is nearly symmetrical and is centered to the southwest of the cone implying that the mountain has fairly uniform magnetic properties and is magnetized in a direction close to that of the present Earth's field.

Modeling Program Input

Two sets of data are needed for input to the modeling routine. First, a topographic model of the source of the magnetic anomaly in question which is developed by polygonizing

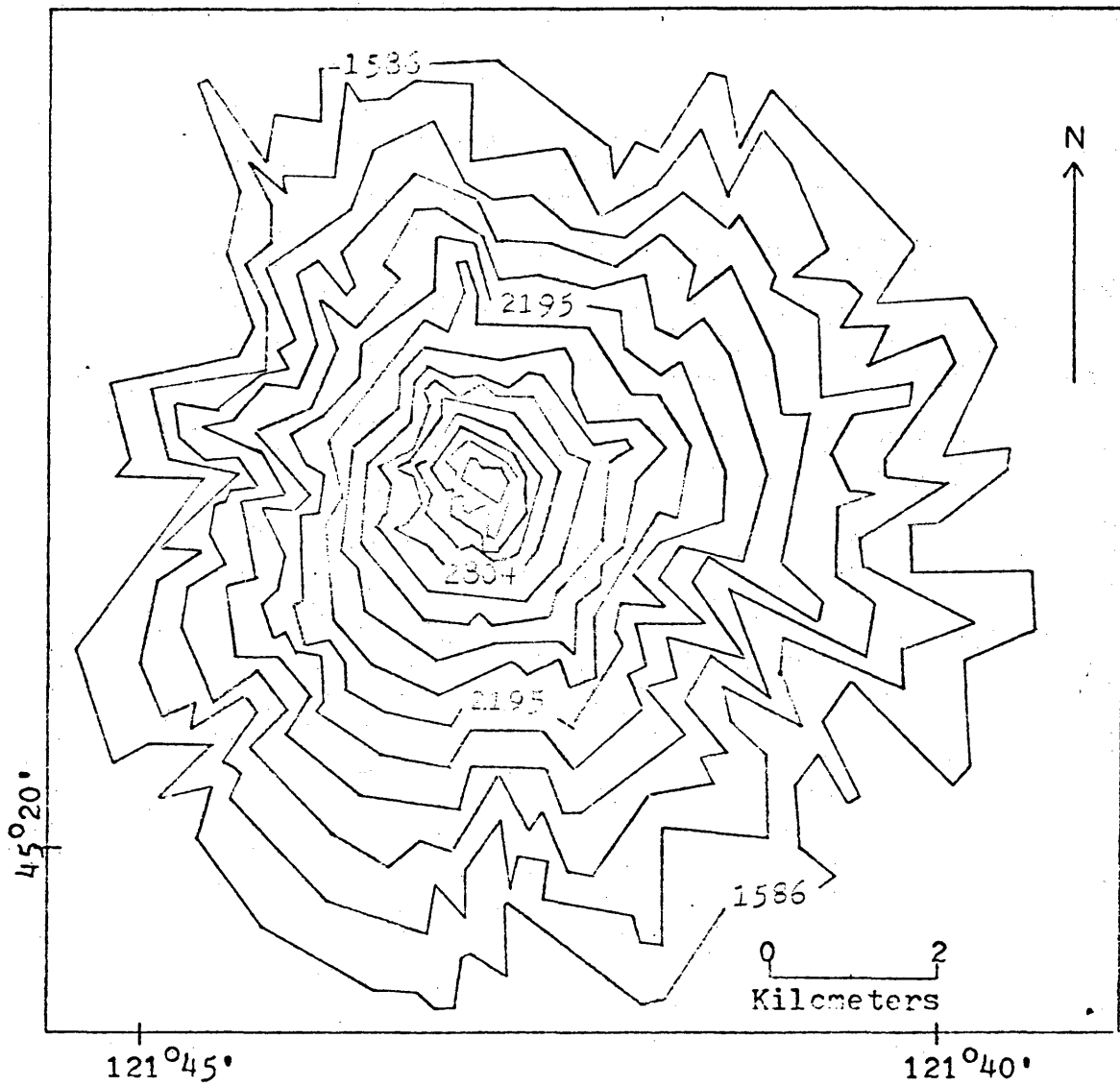
(replacing curved lines with straight lines to form a closed polygonal surface). the elevation contours from a topographic map. Second, the observed aeromagnetic anomaly over the source represented by the polygonized contours.

The source of the observed anomaly is approximated by a topographic model of the mountain (Fig. 8) consisting of 21 polygonal layers with the top of the model at 3414 meters and the base at 1158 meters. The upper five layers are each 61 meters thick and the lower 16 layers are each 122 meters thick. Thinner layers were used near the top to insure a better approximation of the section of the mountain nearest the point of observation since they have the largest effect on the location and shape of the anomaly.

To insure the use of the best possible data as input to the modeling effort the original flight-line data was prepared for input as follows:

1. the IGRF was removed point by point from the total-field flight-line file supplied by the contractor,
- and 2. these ungridded values were projected via a universal transverse mercator projection onto a coordinate system corresponding to that used in creating the topographic model of the mountain; base latitude, $45^{\circ}20'$, and central meridian, $121^{\circ}45'$.

A regional field was then calculated for the integrated



contour interval = 121.8 meters

Figure 8. Topographic model of the Mount Hood cone.

aeromagnetic data. The regional field was calculated, using the equation for a plane, from the USGS program for least-squares surface fitting (Sweeney, 1978). The equation of the calculated regional in nT was:

$$= 28.118063 - 1.061200x - 0.440931y$$

where x and y are distances in kilometers east and north respectively from a point 4.82 kilometers east and 5.32 kilometers north of the model origin. The calculated regional was then removed point by point from the residual flight-line data yielding values for input into the modeling program.

Initial Modeling Results

The results of eight inversions to determine the best-fit magnetization for the entire cone, using various topographic models to approximate the mountain, are summarized in Table 6. The first inversion used a topographic model with base at 1158 meters and top at 3414 meters. Each successive inversion was done by removing another layer from the base of the model. The least-squares fits are evaluated by two commonly used statistical parameters. First, the standard deviation (S) which indicates a better fit as it becomes smaller. Second, the correlation coefficient (R) which has a value, $0 < R < 1$, with $R=1$ indicating an exact fit between the anomaly calculated from the least-squares magnetization and the observed anomaly.

The results presented in Table 6 indicate that the best mathematical model of the mountain consists of 16 layers with top at 3414 meters elevation and the base at 1646 meters elevation. As with the Mount Shasta modeling (Blakely and Christiansen, 1978) the statistical parameters

TABLE 6

Least-Squares Best-Fit Magnetization Inversions

Model	Base	Top	J	I	D	S	R	Datum
1	1158	3414	1.64	77.6	-3.4	19	0.95	-50
2	1280	3414	1.64	76.6	-1.8	19	0.96	-38
3	1402	3414	1.66	75.2	-0.7	18	0.96	-26
4	1524	3414	1.68	73.3	-0.2	18	0.96	-13
5	1646	3414	1.73	70.9	-0.6	17	0.96	0
6	1768	3414	1.82	68.3	-1.7	17	0.96	12
7	1890	3414	1.96	65.4	-2.6	17	0.96	22
8	2012	3414	2.18	62.3	-3.7	18	0.96	31

varied so little from model to model that their use in comparing the models is questionable.

The calculated least-squares magnetization vector for the 16 layer model has a magnitude of 1.73 A/m, inclination (I) of 70.9° and declination (D) of -0.6° . These results, coupled with the relatively good fit ($R=0.96$), indicate that the initial assumptions of uniform direction and intensity of magnetization were reasonable. The calculated magnetization correlates well with the fact that the volcano is relatively young and thus, normally magnetized. As a first approximation one would assume that a volcano built with short term eruptions scattered over the last 100,000 years would have a direction of magnetization close to that

of the geocentric dipole field which at Mount Hood has an inclination of 63.9° and a declination defined as 0° . The small deviation between the calculated direction and the geocentric dipole is quite reasonable as their likely has been long periods of quiescence which may have affected the averaging of the remnant field towards the geocentric dipole. The magnitude of the magnetization (1.73 A/m) although somewhat lower than expected from the laboratory results ($2.8 \pm 1.1 \text{ A/m}$), is still within one standard error of the mean. This difference may be due to the laboratory value being based on surface outcrops which may not be representative of the bulk of the mountain or to some anomalous mass within the mountain which is in disagreement with the initial assumptions of homogeneity.

Inspection of the residual based on the best-fit magnetization (Fig. 9) yields a number of observations. First, although the correlation coefficient indicates an extremely good fit ($R=0.96$), a significant residual ($\pm 30 \text{ nT}$) still exists. Second, the calculated anomaly indicates that the north to northwest section of the mountain (negative residual greater than -30 nT) is either significantly less magnetic or reversed with respect to the south-central portion of the mountain (positive residual greater than 20 nT). Third, there is a recognizable negative gradient in the southeast corner of the residual map.

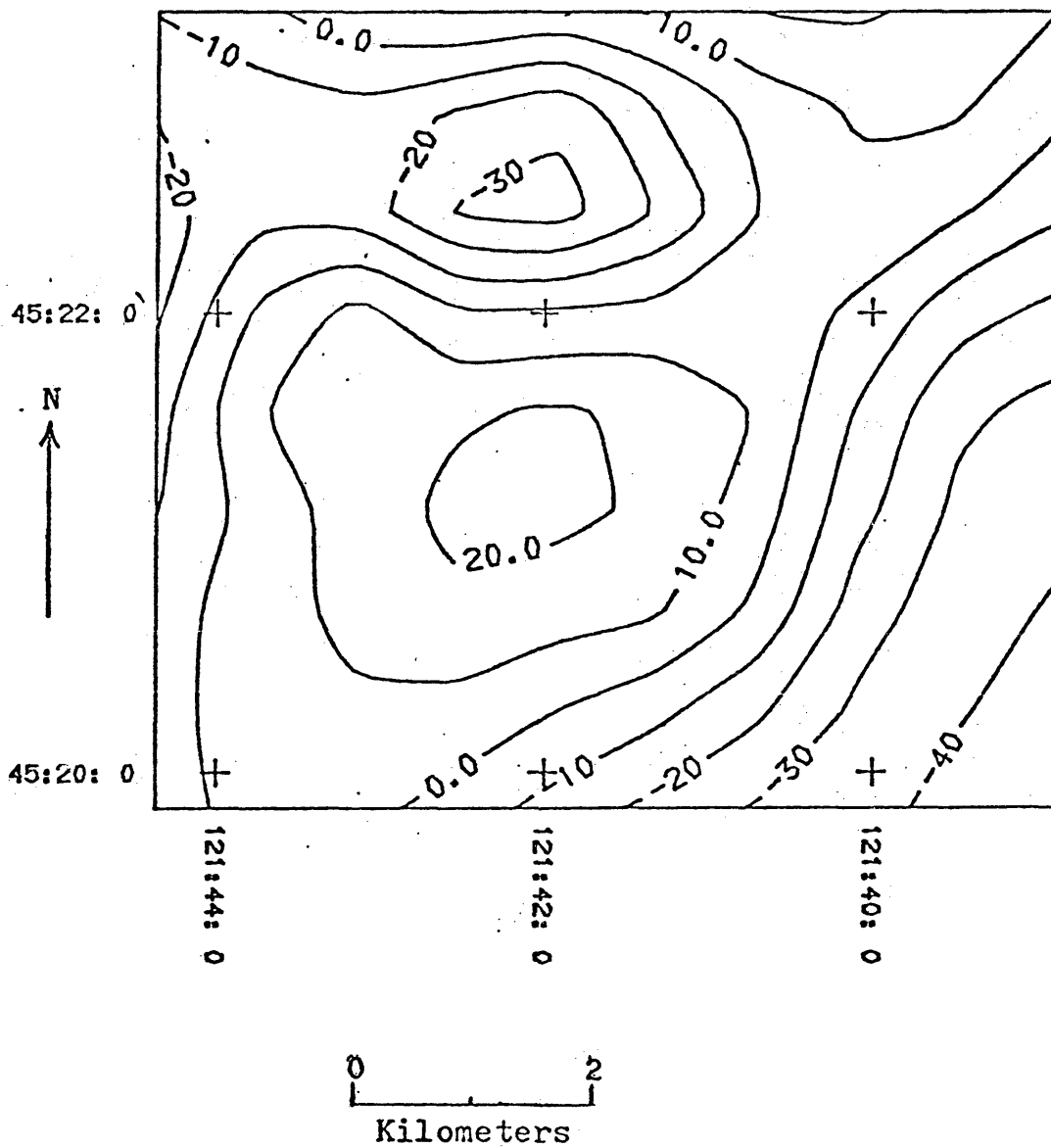


Figure 9. Residual from the 16 layer least-squares best-fit of the Mount Hood cone anomaly ($I=70.9^\circ$, $D=-0.6^\circ$).

The Refined Model

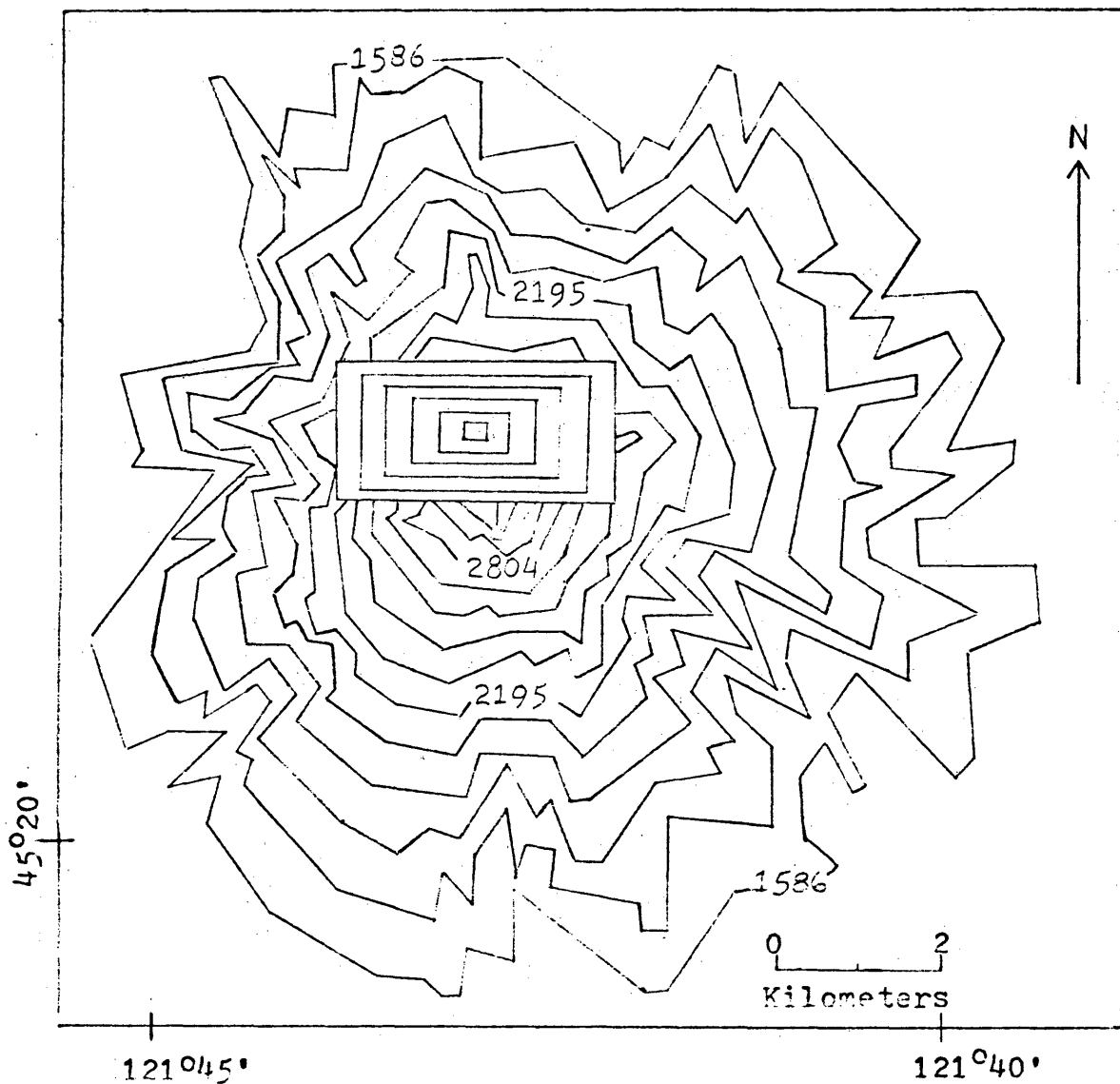
Modeling to obtain a more refined geologic-magnetic model of the Mount Hood cone was done using a combination of the forward and inverse least-squares modeling routines. The refined model was based on the residual from the 16 layer least-squares fit of the entire cone. The geologic and magnetic laboratory data established two possible causes for the difference in magnetization, between the northwest and south-central portions of the mountain, indicated in the residual. First, the crater area which exhibits exceptionally high remnant magnetizations (13.66 A/m) and second, the remains of the Sandy Glacier Volcano on the northwest slope of Mount Hood which may have a reversed component of remnant magnetization.

Simple forward models of a cap or plug at the crater area indicated that the addition of highly magnetized, normally polarized material in this area would not yield the desired effect of reducing the residual anomalies. The addition of a cap or plug, although reducing the positive residual over the south-central portion of the mountain, significantly increased the negative residual in the northwest. Therefore, it is assumed that the high remnant magnetizations obtained from the laboratory analyses of rocks from the crater area (Table 2) are restricted to a small

quantity of material which does not contribute significantly to the observed magnetic field pattern.

A simple pyramidal model (Fig. 10) with base at 1646 meters and top at 2743 meters was used as an approximation of the Late Pliocene, Sandy Glacier Volcano. The size, position and magnetization (6.50 A/m) of the model was determined by calculating the magnetic field due to a first approximation model, with magnetization direction reversed from the geocentric dipole ($I=-63.9^\circ$, $D=180.0^\circ$). The field due to this first approximation model was compared to the magnitude and position of the least-squares best-fit residual's (Fig. 9) negative anomaly. The model was adjusted and the process repeated until a reasonable approximation of the residual anomaly's characteristics was obtained.

Reversed polarity was assumed in modeling the Sandy Glacier Volcano for three reasons. First, the 16 layer best-fit residual (Fig. 9) indicates relatively less magnetic material in the northwest than elsewhere on the mountain. Second, Wise (1969) dates the Sandy Glacier Volcano as Late Pliocene and if it conforms to the general trend of Late Pliocene volcanics in the area it would be expected to have a reversed polarity. Third, the laboratory results (Table 3) indicate no consistent direction for the remnant magnetization of the Sandy Glacier Volcano samples and thus, they do not



contour interval (main cone) = 121.8 meters
 contour interval (Sandy Glacier Volcano) = 182.7 meters

Sandy Glacier Volcano: top = 2743 meters elevation
 bottom = 1646 meters elevation

Figure 10. Projection of the Sandy Glacier Volcano model onto the topography of the Mount Hood cone.

contradict the reversed polarity hypothesis.

The next phase of the Mount Hood cone modeling consisted of 3 distinct steps. First, the calculated magnetic field due to the adjusted Sandy Glacier Volcano model was subtracted from the observed magnetic field over the cone, yielding an input field for the modeling routine. Second, the input field was used to calculate a new least-squares best-fit magnetization vector for the cone as a whole and thus, a second residual map. Third, the residual map and magnetization vector resulting from this inversion was inspected and used as a basis for adjusting the Sandy Glacier Volcano model. The process is repeated using the new version of the Sandy Glacier Volcano model until a satisfactory residual map and magnetization vector is obtained.

The refined model of the Mount Hood cone which results from the above process shows a significant improvement over the 16 layer best-fit model (Fig. 9). The residual (Fig. 11) resulting from the refined model, except for a few edge effects, is restricted to values between ± 10 nT, less than 5 percent of the observed anomaly's magnitude of 243 nT. The correlation coefficient and standard deviation are >0.995 and 9 nT respectively compared to 0.96 and 17 nT for the 16 layer best-fit of the entire cone. The calculated least-squares magnetization vector for the bulk of the cone

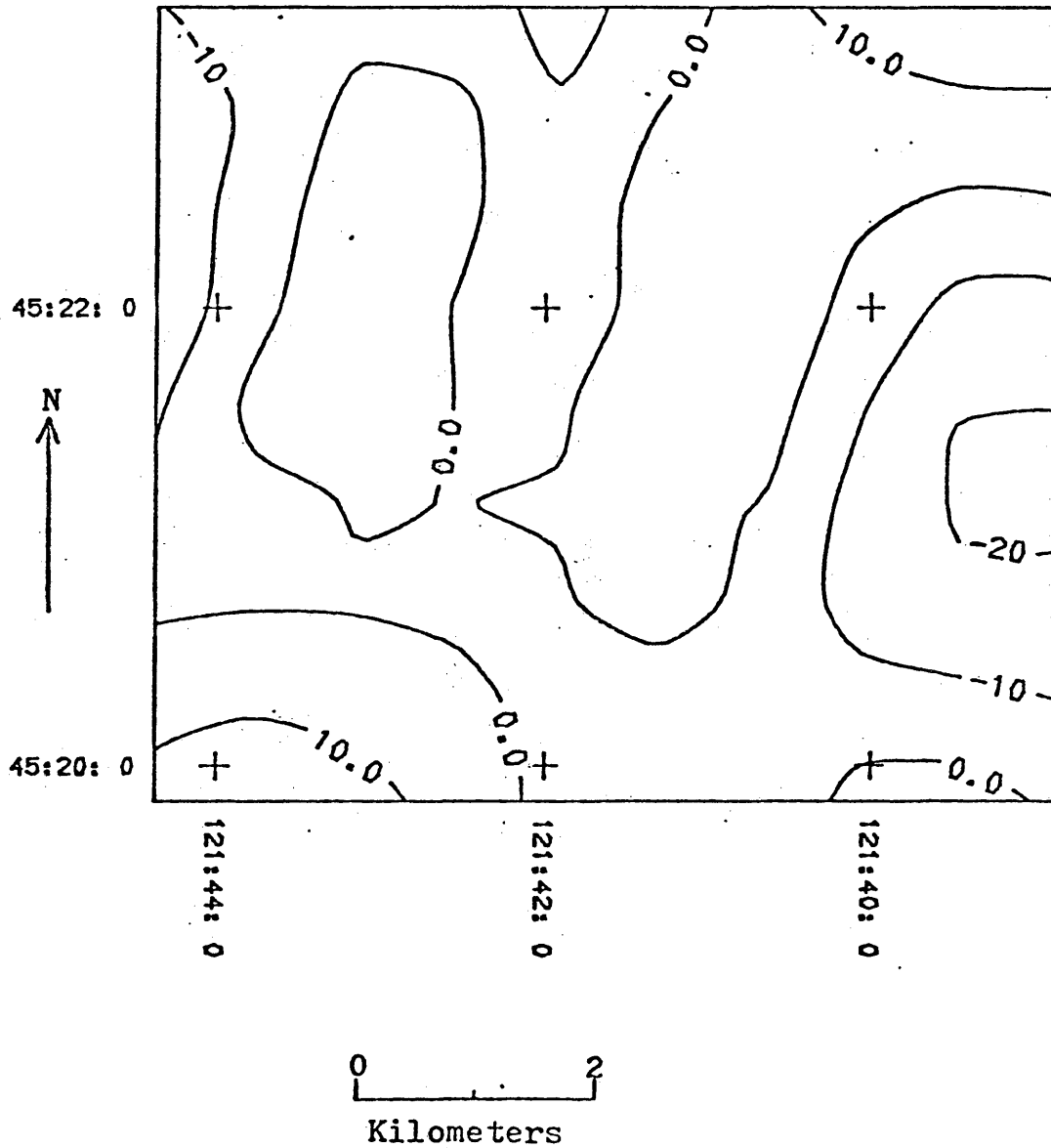


Figure 11. Residual from the refined modeling of the Sandy Glacier Volcano ($I=-63.9^\circ$, $D=180.0^\circ$, and $J=6.5$ A/m) and Mount Hood cone ($I=80.0^\circ$, $D=28.3^\circ$, and $J=2.9$ A/m).

has a magnitude of 2.9 A/m, inclination of 80.0° and declination of 28.3° which yields a magnitude of magnetization, with reversed polarity, of 3.9 A/m for the Sandy Glacier Volcano. This rather high value of reversed magnetization for the Sandy Glacier Volcano was not expected from the results of the laboratory work (Table 3). However, the limited outcrops of this old volcano may not have allowed for a definitive sampling of the basaltic rocks (which would be expected to have higher magnetizations) composing it.

The calculated magnetization of 2.9 A/m for the bulk of the Mount Hood cone correlates exceptionally well with the average value of 2.8 A/m obtained from the laboratory samples. The calculated magnetization direction ($I=80.0^\circ$, $D=28.3^\circ$) for the Mount Hood cone is within 11° of the Earth's present field ($I=68.5^\circ$, $D=20.3^\circ$). This difference in magnetization direction is probably the result of the original modeling assumptions. First, the simplifying assumptions of uniform direction and intensity of magnetization for both the Mount Hood cone and the Sandy Glacier Volcano are not accurate in detail. Second, the position, size, and especially the shape of the pyramidal model representing the Sandy Glacier Volcano are probably

not accurate. Third, the direction of magnetization used to forward model the Sandy Glacier Volcano is only a best guess approximation.

To evaluate the effect these estimates might have on the modeling a simple two phase calculation was attempted. First, the original 3 step modeling process was used. However, the forward modeling calculated the field due to the Mount Hood cone and a best-fit least-squares magnetization was found for the Sandy Glacier Volcano of figure 10. The forward modeling was done by assigning the Mount Hood cone the direction of magnetization of the earth's present field ($I=68.5^\circ$, $D=20.3^\circ$) with a magnitude equal to that found for the best refined model ($J=2.9$ A/m, Fig. 11). Results of the inversion of the Sandy Glacier Volcano ($I=-38.2^\circ$, $D=195^\circ$, and $J=6.9$ A/m) indicated that some adjustment might still be needed in the parameters used in representing the Sandy Glacier Volcano. The second step, employed the use of the original 3 step process for refining the Mount Hood cone model but with the parameters of the Sandy Glacier Volcano adjusted ($I=-55.0^\circ$, $D=190.0^\circ$, and $J=6.9$ A/m).

The residual resulting from this final modeling effort (Fig. 12) is the result of a Mount Hood cone model with inclination of 76.4° , declination of 27.6° and magnitude of magnetization of 2.8 A/m. The desired effect, changing the

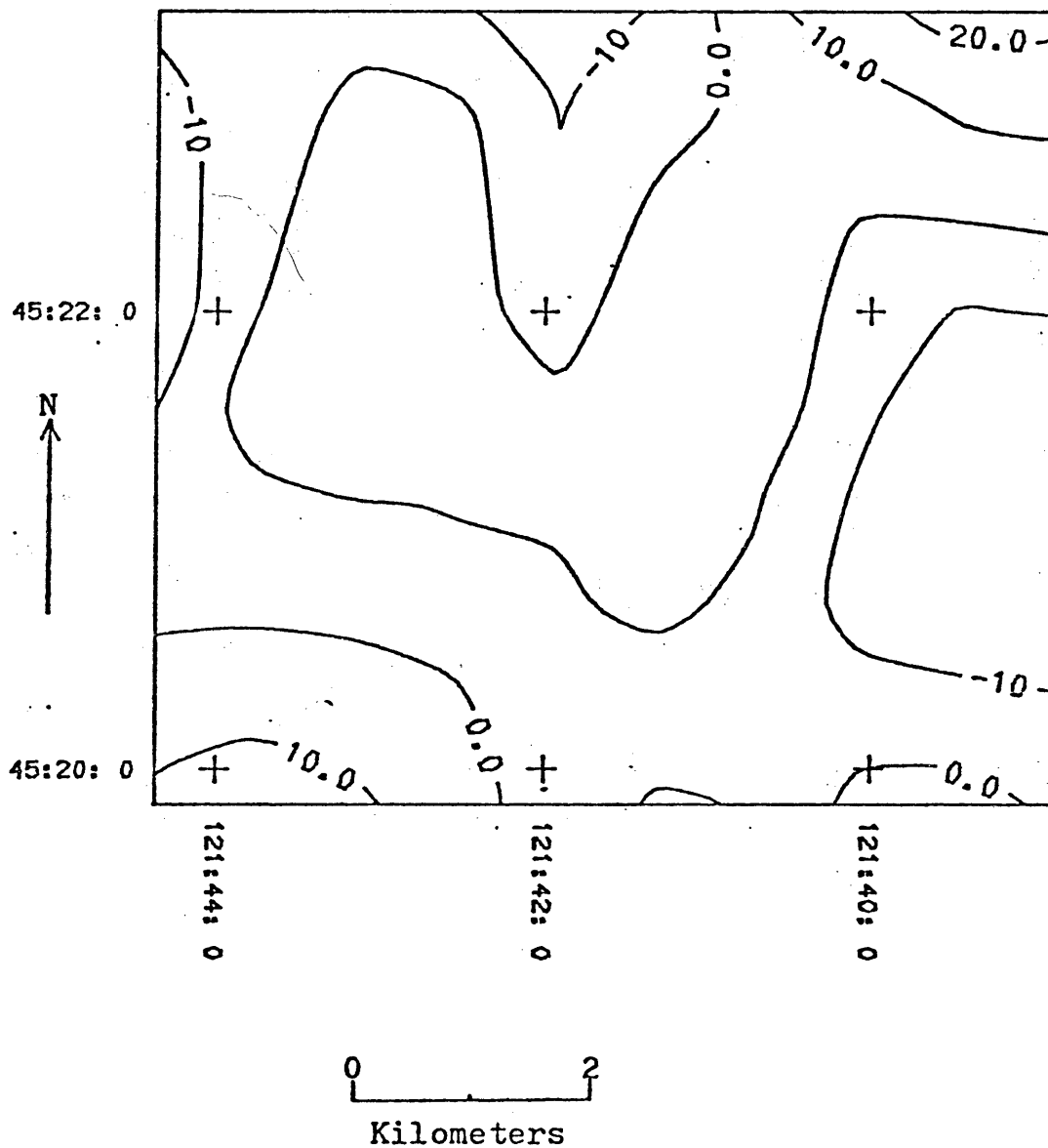


Figure 12. Residual from the refined modeling of the Sandy Glacier Volcano ($I=-55.0^{\circ}$, $D=190.0^{\circ}$, and $J=6.9$ A/m) and the Mount Hood cone ($I=76.4^{\circ}$, $D=27.6^{\circ}$, and $J=2.8$ A/m).

magnetization direction of the model closer to the present Earth's field, seems to have been achieved without significantly worsening the residual pattern and while retaining the same good quality statistical fit parameters ($R > 0.995$, $S = 9$).

From the results of this final model it is evident that a change in some or possibly all of the magnetization and geometric parameters for the Sandy Glacier Volcano might improve the results of the modeling by at least a small amount. However, without further geophysical or borehole data on which to base the parameter changes and realizing the non-unique nature of potential fields, attempts to refine the model further would probably be superfluous.

The exceptionally good residual and statistical parameters, combined with the reasonable direction of magnetization for the Mount Hood cone as a whole, indicates that the Sandy Glacier Volcano is the chief cause of inhomogeneity in the Mount Hood volcanic cone. Although other inhomogeneities undoubtedly occur they are probably too small to be identified in the high-level aeromagnetic pattern.

The modeling results also indicate that approximately 10 percent of the approximately 37.5 cubic kilometers of Mount Hood volcanics above 1646 meters elevation are due to the Late Pliocene Sandy Glacier Volcano. This large amount of

uneroded material at such high elevations may indicate that the Sandy Glacier Volcano is much younger than the potassium-argon date of 3.2 million years which is referred to by Wise (1969).

CONCLUSIONS

In assessing the goals of this study we find that the first goal, of increasing our knowledge about the geologic structure of the survey area, was obtained through the support this study lends to the geologic interpretations of Wise (1969) and in the development of a geologic-magnetic model of the Mount Hood volcanic cone.

The quantitative modeling of the Mount Hood volcanic cone yields two significant facts. First, the main bulk of the volcano is composed of magnetically similar andesites magnetized ($I=80.0^\circ$, $D=28.3^\circ$, and $J=2.9$ A/m) in a direction close to the present Earth's field. Second, there exists one major exception to this homogeneity, the Sandy Glacier Volcano which underlies the northwest flank of Mount Hood and is magnetically reversed from the main bulk of the Mount Hood andesites.

It was also found that approximately one-tenth of the volcanic deposits comprising the Mount Hood cone may be the result of outpourings of the Sandy Glacier Volcano. This may indicate that the Sandy Glacier Volcano is much younger than the 3.2 million years referred to by Wise (1969). The second goal, of evaluating the geothermal potential of the survey area was left unsolved since no indications of

hydrothermal alteration were found. Structure at depth that might indicate likely hydrothermal systems was in general obscured since it was found that the aeromagnetic anomaly pattern was controlled to a large extent by the topographic expression of the Cenozoic volcanics which cover the survey area. Therefore, until a method can be found to remove the topographic effects from the magnetic anomaly pattern the evaluation of the area's geothermal potential must be left to other geophysical or geochemical methods.

BIBLIOGRAPHY

- Blakely, R.J. and Christiansen, R.L., 1978, The magnetization of Mount Shasta and implications for virtual geomagnetic poles determined from seamounts: Journal of Geophysical Research, v. 83, n. B12, p. 5971-5978.
- Bott, M.H.P., 1963, Two methods applicable to computers for evaluating magnetic anomalies due to finite three-dimensional bodies: Geophysical Prospecting, v. 11, p. 292-299.
- Fuller, B.D., 1967, Two-dimensional frequency analysis and design of grid operators: Mining Geophysics, v. 2, SEG, Tulsa, Oklahoma, p. 658-708.
- Hildebrand, T.G., 1978, personal communication.
- Lourenco, J.S., 1972, Analysis of three-component magnetic data, Ph.D. thesis, University of California, Berkeley, California.
- Plouff, Donald, 1975, Derivation of formulas and FORTRAN programs to compute magnetic anomalies of prisms: Natl. Tech. Inf. Service, no. PB-243-525, U.S. Dept. of Commerce, Springfield, Virginia, 112 p.
- Sweeney, R.E., 1978, personal communication.
- Talwani, Manik, 1965, Computation with the help of a digital computer of magnetic anomalies caused by bodies of arbitrary shape: Geophysics, v. 30, p. 797-817.
- Vacquier, V. 1962, A machine method for computing the magnitude and direction of magnetization of a uniformly magnetized body from its shape and magnetic survey: Benedum Symp. on Paleomagnetism, edited by T. Nagata, Univ. of Pittsburgh, p. 123-137.
- Webring, M.W., 1978, personal communication.
- White C.M., 1978, Geology and geochemistry of Mount Hood volcano: unpublished report to the Oregon Dept. of Geol. and Min. Ind., 4p.

Wise, W.S., 1969, Geology and petrology of the Mount Hood area: a study of high cascade volcanism: Bull. Geol. Soc. of Amer., v. 80, p. 969,1006.

Wise, W.S., 1977, A geologic appraisal of geothermal energy at Mount Hood, Oregon: unpublished report to the Oregon Dept. of Geol. and Min. Ind., 5p.

Wise, W.S., 1979, personal communication.

GEOLOGY OF THE MT. HOOD AREA, OREGON

Explanation

- QUATERNARY AND RECENT**
- Qal Alluvium and mudflow deposits, mostly in river valleys
 - Qgl Glacial moraines on Mt. Hood, from active glaciers; in valleys around Mt. Hood, from Fraser Glaciation
 - Qtl Talus and landslides
 - Qbc Basalts and andesites, some from vents satellite to Mt. Hood, and Recent flow. Cinder cones
 - Qhm Mt. Hood andesite flows
 - Qhc Mt. Hood clastic debris, largely pyroclastic but on surface much post-glacial redistributed detritus
 - Qhb Harshlands andesite plugs and flows
- PLIOCENE**
- Puv Upper Pliocene basalts and andesite; 80% andesite in all parts of the area except near Bull Run Lake
 - Pis Lateral Hill and Still Creek intrusions
 - Pvl Lower Pliocene basalts and andesites; 90% andesite in all parts of the area except on Blue Ridge
 - Pil Lower Pliocene andesitic plugs and shallow intrusions
- MIOCENE**
- Mz Deltas formation, pyroclastic and water-laid volcanic debris with a few flows
 - Msd Shoshonean Formation, pyroclastic with some water-laid volcanic debris, many interbedded flows near top
 - Mhb Yachima Basalt

M 50 K-Ar age date in millions of years



Geology by W. S. Wise, 1968
1962-65 mapped on 1:25,000 sheets



PLATE 1
T-2168
GUY FLANAGAN

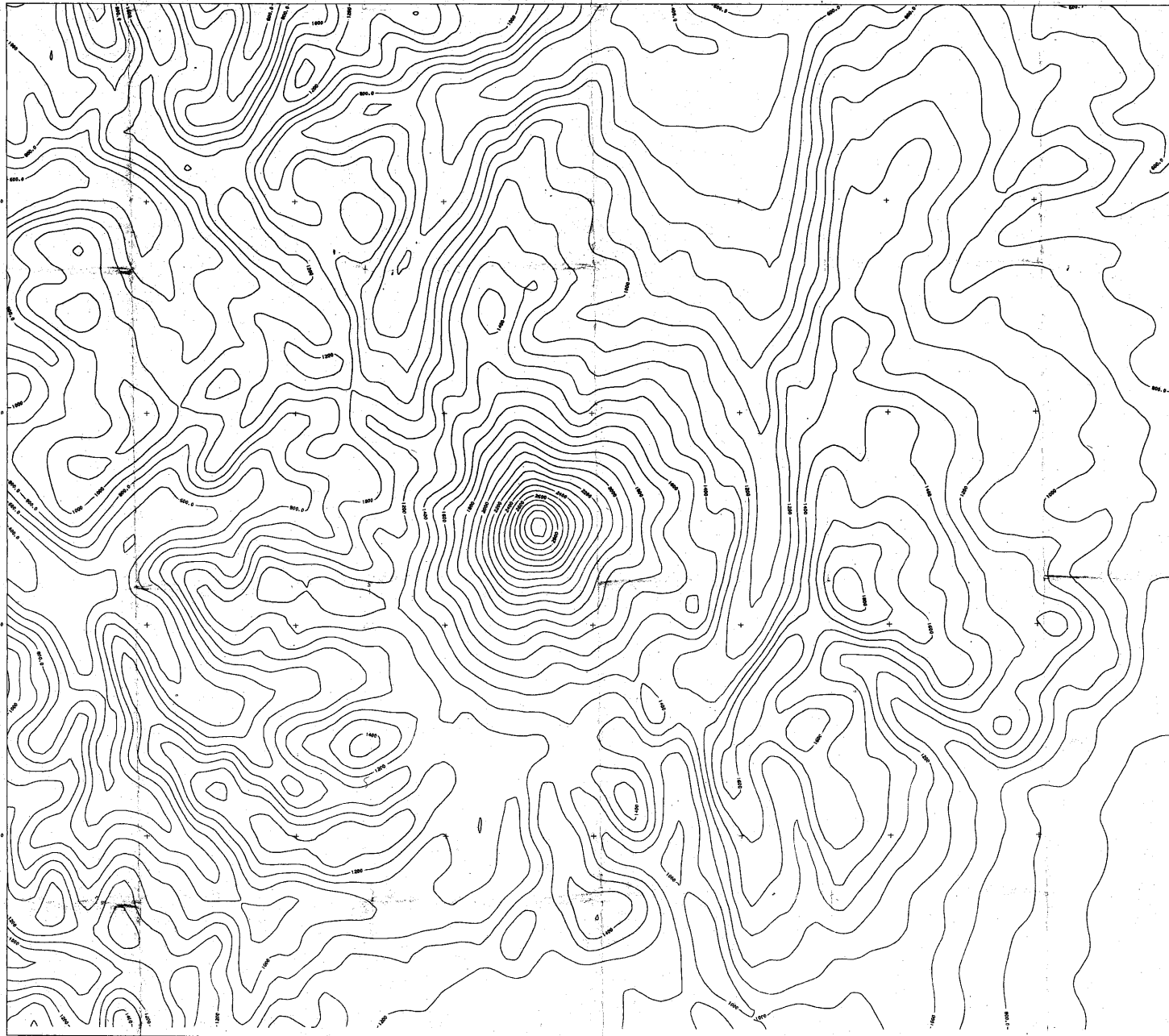
Index to 7 1/2° Quadrangles

	MILL RUN LAKE	CAMPBELL RIDGE	BOB BUTTE
INDOCHINA	GOVERNMENT CAMP	TIMBERLINE LODGE	BADGER LAKE

COLORADO SCHOOL OF MINES LIBRARY
 01880022844905

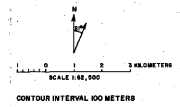
ARTHUR LEVINE LIBRARY
 COLORADO SCHOOL OF MINES
 GOLDEN, COLORADO 80401





UNIVERSITY MICROFILMS
SERIALS ACQUISITION
300 N ZEEB RD
ANN ARBOR MI 48106
PLATE 10
GUY FLANAGAN
COLORADO SCHOOL OF MINES
THESIS: T-2168

**MOUNT HOOD OREGON
TOPOGRAPHY**



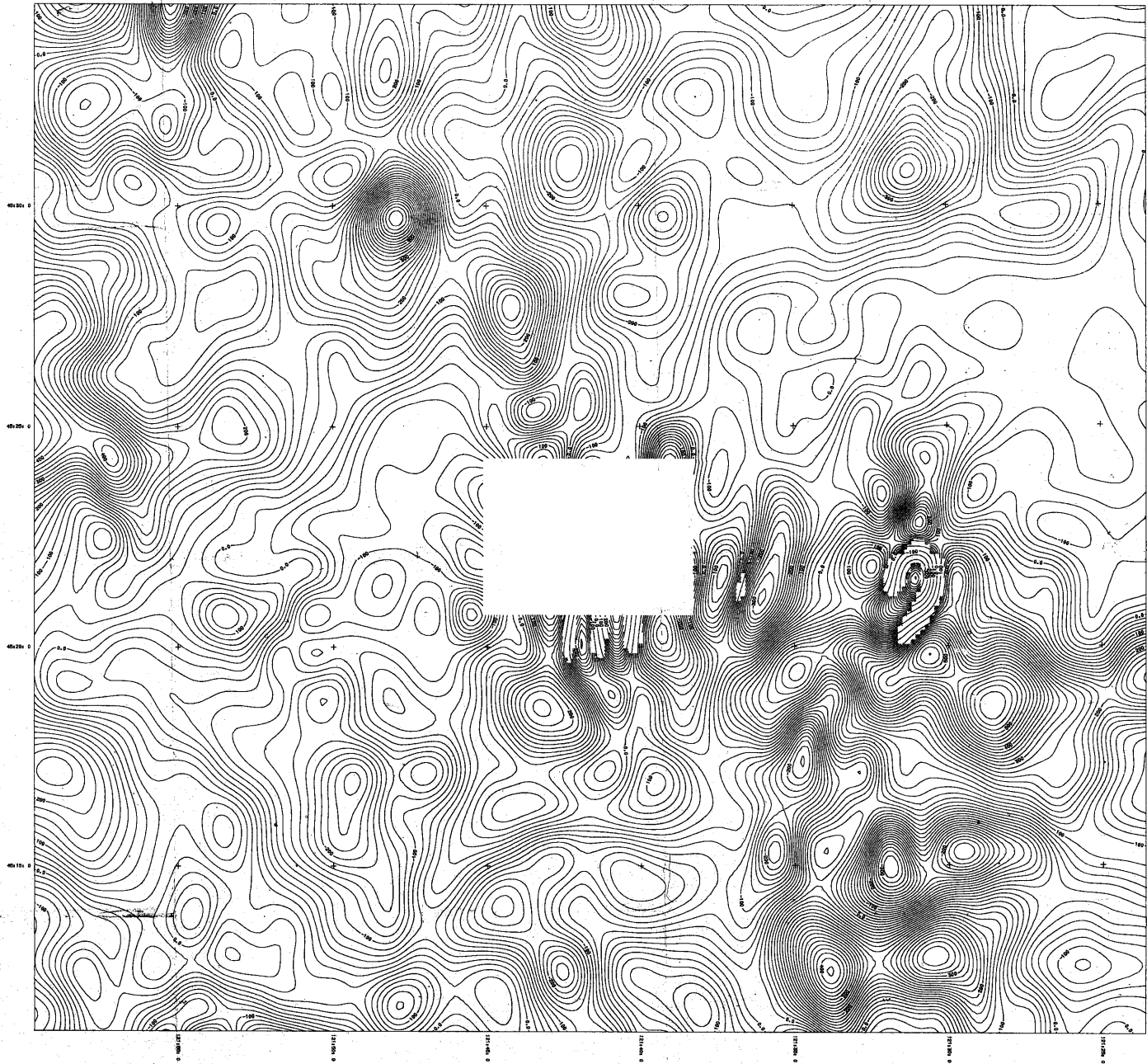
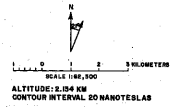
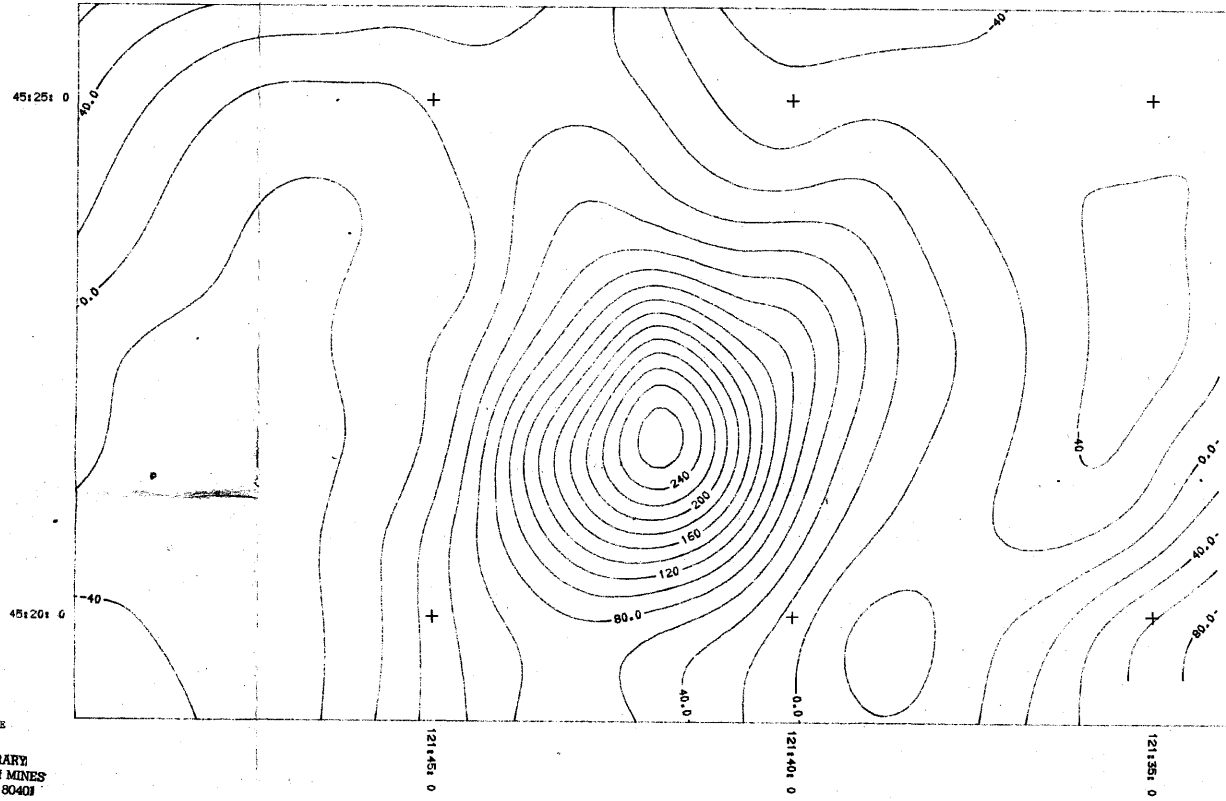


PLATE 2
GUY FLANAGAN
COLORADO SCHOOL OF MINES
THESIS: T-2168

MOUNT HOOD OREGON
LOW LEVEL AEROMAGNETICS

UNIVERSITY OF COLORADO
LIBRARY
1000 UNIVERSITY BLVD.
BOULDER, COLORADO 80502

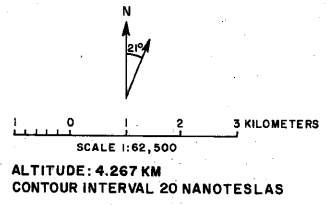


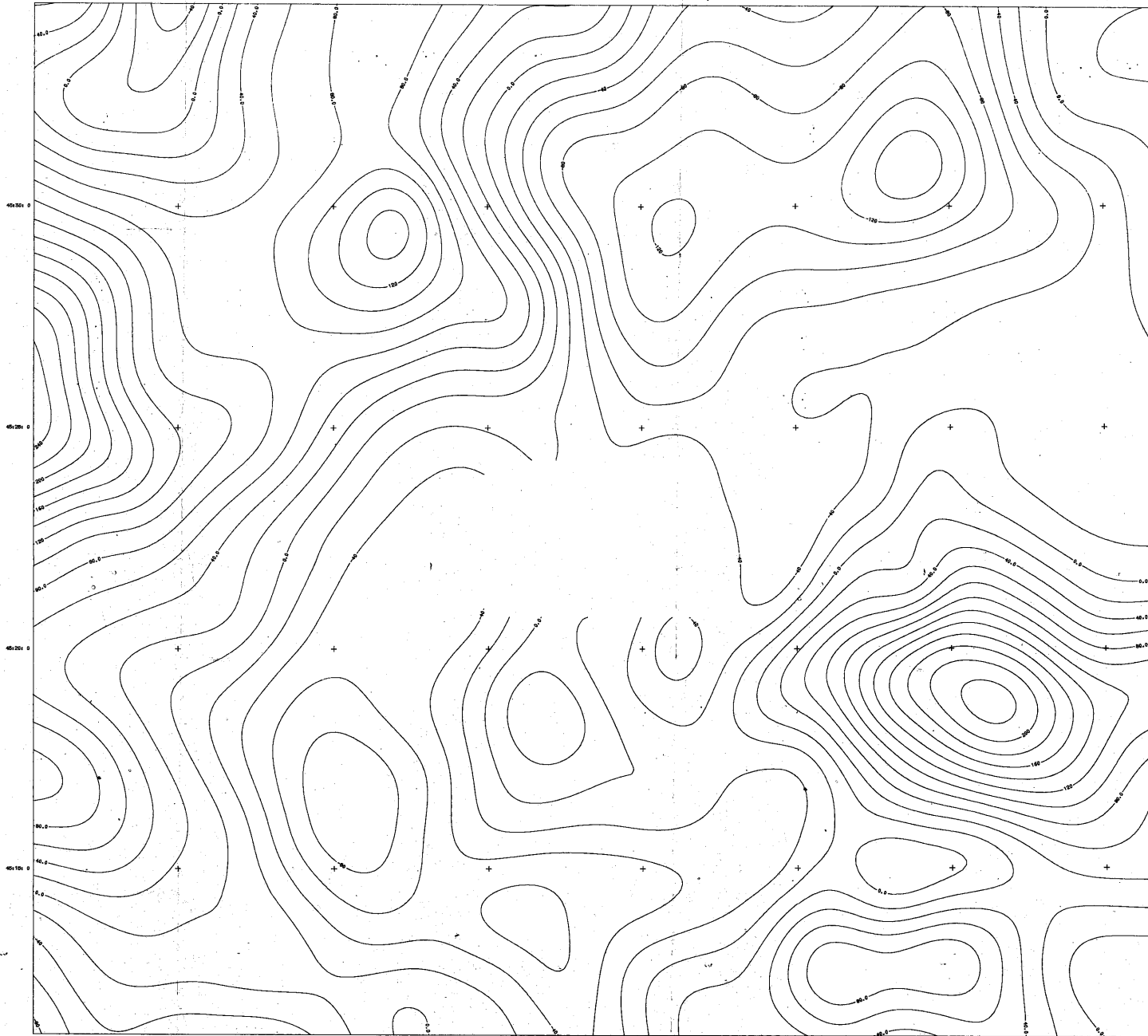


CLOSED RESERVE
ARTHUR LAKES LIBRARY
COLORADO SCHOOL OF MINES
GOLDEN, COLORADO 80401

PLATE 3
GUY FLANAGAN
COLORADO SCHOOL OF MINES
THESIS: T-2168

**MOUNT HOOD OREGON
HIGH LEVEL AEROMAGNETICS**

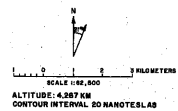




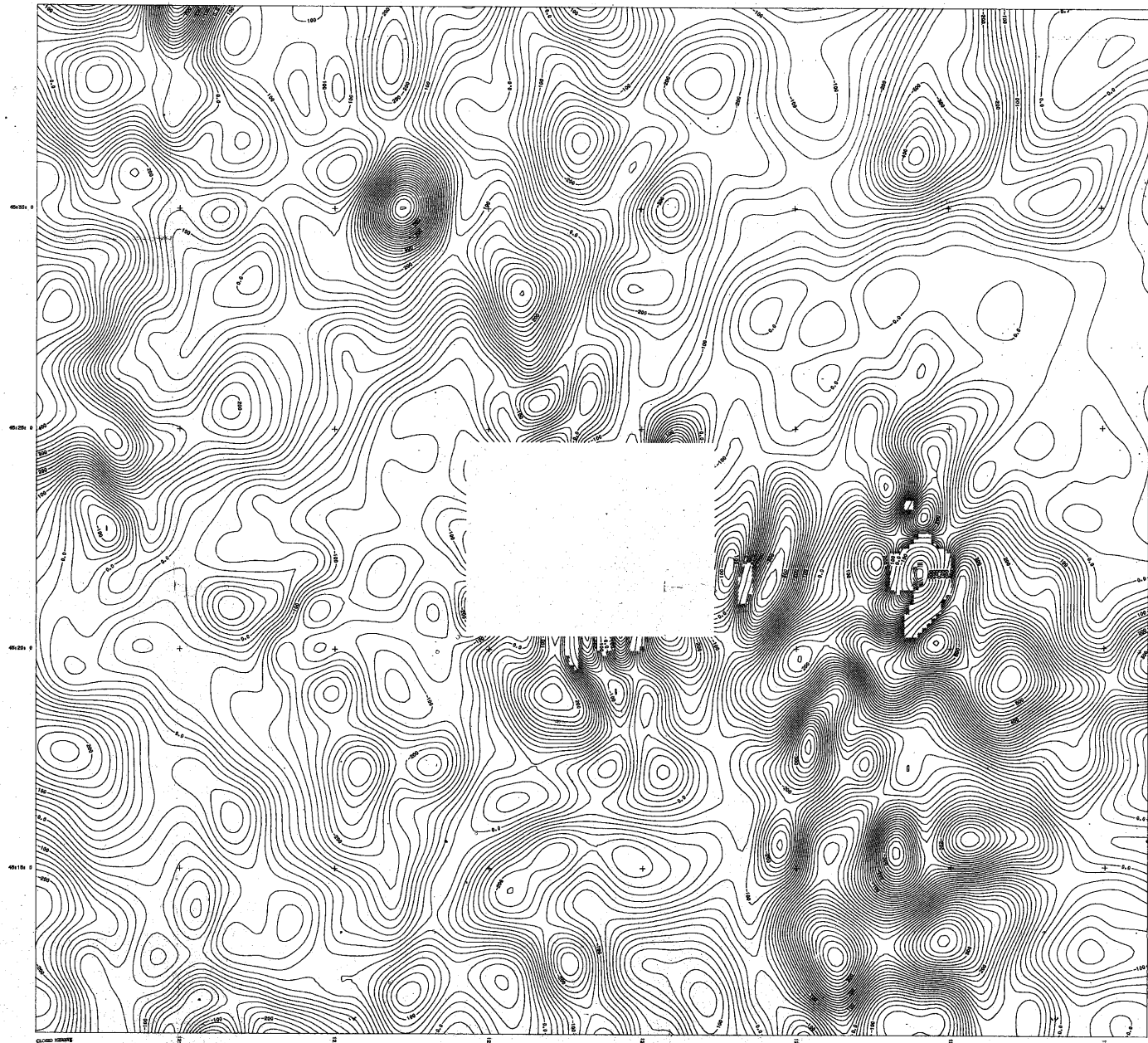
COLORADO STATE
UNIVERSITY
DEPARTMENT OF GEOSCIENCE
GOLDEN, COLORADO 80401

PLATE 4
GUY FLANAGAN
COLORADO SCHOOL OF MINES
THESIS: T-2168

MOUNT HOOD OREGON
LOW LEVEL AEROMAGNETICS,
UPWARD CONTINUED

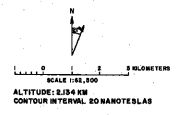


134800228480

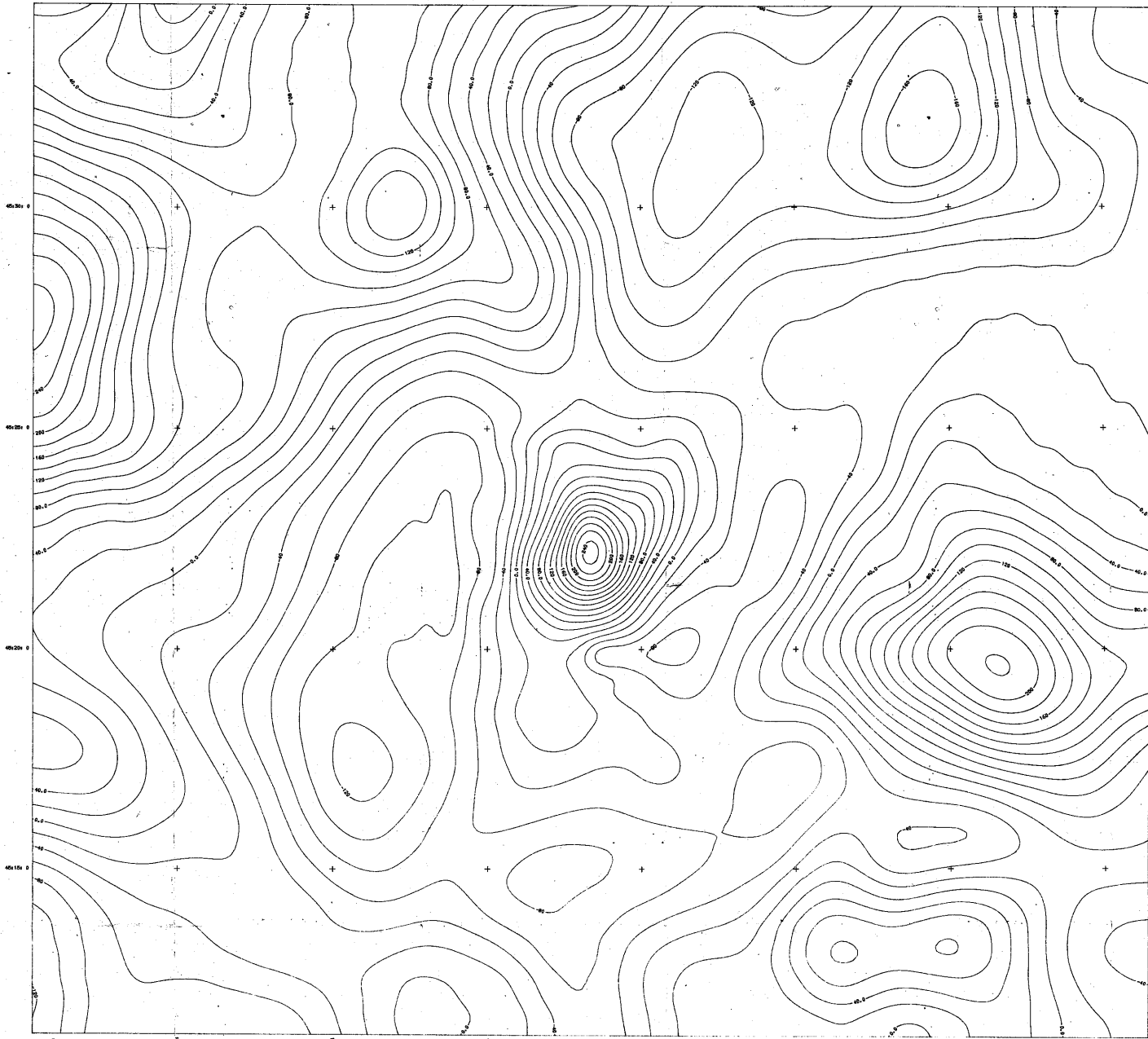


UNITED STATES
GEOLOGICAL SURVEY
COLORADO SECTION OF MINES
GUY FLANAGAN
COLORADO SCHOOL OF MINES
THESIS: T-2168

MOUNT HOOD OREGON
LOW LEVEL AEROMAGNETICS,
REDUCED-TO-THE-POLE



U.S. GEOLOGICAL SURVEY



U.S. GEOLOGICAL SURVEY
ARTHUR C. WOOD
COLORADO SCHOOL OF MINES
GUY FLANAGAN
PLATE 7
GUY FLANAGAN
COLORADO SCHOOL OF MINES
THESIS: T-2168

**MOUNT HOOD OREGON
INTEGRATED AEROMAGNETICS,
REDUCED-TO-THE-POLE**

